

# Damping and vibration response of viscoelastic smart sandwich plate reinforced with non-uniform Graphene platelet with magnetorheological fluid core

Arameh Eyvazian<sup>\*1</sup>, Abdel Magid Hamouda<sup>1</sup>, Faris Tarlochan<sup>1,2</sup>,  
Saeid Mohsenizadeh<sup>3</sup> and Ali Ahmadi Dastjerdi<sup>4</sup>

<sup>1</sup> Mechanical and Industrial Engineering Department, College of Engineering, Qatar University, P.O. Box 2713, Doha, Qatar

<sup>2</sup> Qatar Transportation and Traffic Safety Center, College of Engineering, Qatar University, Qatar

<sup>3</sup> School of Mechanical Engineering, Faculty of Engineering, Universiti Teknologi Malaysia, 81310, Johor Bahru, Malaysia

<sup>4</sup> Mechanical Engineering Department, Delft University of Technology, Delft, The Netherlands

(Received July 29, 2019, Revised October 16, 2019, Accepted October 21, 2019)

**Abstract.** This study considers the instability behavior of sandwich plates considering magnetorheological (MR) fluid core and piezoelectric reinforced facesheets. As facesheets at the top and bottom of structure have piezoelectric properties they are subjected to 3D electric field therefore they can be used as actuator and sensor, respectively and in order to control the vibration responses and loss factor of the structure a proportional-derivative (PD) controller is applied. Furthermore, Halpin-Tsai model is used to determine the material properties of facesheets which are reinforced by graphene platelets (GPLs). Moreover, because the core has magnetic property, it is exposed to magnetic field. In addition, Kelvin-Voigt theory is applied to calculate the structural damping of the piezoelectric layers. In order to consider environmental forces applied to structure, the visco-Pasternak model is assumed. In order to consider the mechanical behavior of structure, sinusoidal shear deformation theory (SSDT) is assumed and Hamilton's principle according to piezoelectricity theory is employed to calculate motion equations and these equations are solved based on differential cubature method (DCM) to obtain the vibration and modal loss factor of the structure subsequently. The effect of different factors such as GPLs distribution, dimensions of structure, electro-magnetic field, damping of structure, viscoelastic environment and boundary conditions of the structure on the vibration and loss factor of the system are considered. In order to indicate the accuracy of the obtained results, the results are validated with other published work. It is concluded from results that exposing magnetic field to the MR fluid core has positive effect on the behavior of the system.

**Keywords:** vibration and loss factor analysis; sinusoidal shear deformation theory; visco-piezoelectric structure; PD controller; magnetorheological fluid; graphene platelets

## 1. Introduction

MR fluids are high-tech materials that can shift their phase from liquid to solid under external magnetic field. In this kind of fluid, the viscosity changes remarkable to the point of becoming a viscoelastic solid when the magnetic field is exposed to the fluid. It is noted that, smart control of MR fluid between top and bottom facesheets can be useful in order to control the behavior of system. In this paper, PD controller for smart control of vibration in MR fluids integrated by piezoelectric facesheets as sensor and actuator is applied.

There are many researches have been presented in the field of sandwich plates with MR core. A model was developed by Wang *et al.* (2001) to study dynamical modelling of the chain structure formation in electrorheological fluids. Damping and vibration analysis of polar orthotropic annular plates with ER treatment was

introduced by Yeh (2009). Yeh (2011) studied free vibration analysis of rotating polar orthotropic sandwich annular plate with electrorheological (ER) fluid core layer. Magnetorheological visco-elastomer and its application to suppressing micro-vibration of sandwich plates were studied by Ying *et al.* (2011). Yeh (2013) investigated the vibration behavior of sandwich rectangular plates with MR elastomer damping. Aguib *et al.* (2014) carried out the dynamic behavior analysis of a MR elastomer sandwich plate. The dynamic stability of a rotating three layered symmetric sandwich beam with magnetorheological elastomer (MRE) core and conductive skins subjected to axial periodic loads was investigated by Nayak *et al.* (2014) using finite element method (FEM). MalekzadehFard *et al.* (2015) studied free vibration and buckling analyses of cylindrical sandwich panel with MR fluid layer. In this research the effects of magnetic field on loss factors and buckling loads according to the first four mode shapes are analyzed. Long-term stable MR fluid brake for application in wind turbines was reported by Güth and Maas (2016). Eshaghi *et al.* (2016) presented analytical and experimental free vibration analysis of multi-layer MR-fluid circular plates under varying magnetic flux. Vibration analysis of a

\*Corresponding author, Ph.D. Student,  
E-mail: [arameh.eyvazian@gmail.com](mailto:arameh.eyvazian@gmail.com)

rotating MR tapered sandwich beam was introduced by Navazi *et al.* (2017). The dynamic mechanical properties of magnetorheological plastomers (MRPs) were studied by Xu *et al.* (2018) applying a Split Hopkinson Pressure Bar (SHPB) equipped with an electromagnetic accessory.

Vibration analysis of sandwich structures has been discovered by several researchers. Through experiments and numerical simulations, free vibration behaviors of carbon fiber reinforced composite (CFRC) lattice-core sandwich cylinder (LSC) were studied by Han *et al.* (2015) under different boundary conditions. Nguyen *et al.* (2015) discovered a refined higher-order shear deformation theory for bending, vibration and buckling analysis of functionally graded sandwich plates. Adiyaman *et al.* (2015) surveyed analytical and finite element solution of a receding contact problem. Yaylacı and Birinci (2015) discovered analytical solution of a contact problem and comparison with the results from FEM. A high order theory was developed by Sadeghpour *et al.* (2016) to study the free vibration response of a debonded curved sandwich beam. Buckling analysis of functionally graded carbon nanotube reinforced composite (FGCNTRC) cut out plate using domain decomposition method and orthogonal polynomials was analyzed by Jamali *et al.* (2016). Nonlinear transient analysis of smart laminated composite plate integrated with PVDF sensor and AFC actuator was studied by Mahapatra (Singh *et al.* 2016). Adiyaman *et al.* (2016) investigated receding contact problem between a functionally graded layer and two homogeneous quarter planes. The dynamic response and the active vibration control behavior of various FGCNTRC rectangular plates was investigated by Sharma *et al.* (2016) numerically instrumented with piezoelectric sensor and actuator layers. Katariya *et al.* (2017a) evaluated Enhancement of thermal buckling strength of laminated sandwich composite panel structure embedded with shape memory alloy fiber. Chen *et al.* (2017) introduced vibration and stability of initially stressed sandwich plates with FGM face sheets in thermal environments. Prediction of nonlinear eigenfrequency of laminated curved sandwich structure using higher-order equivalent single-layer theory was analyzed by Katariya *et al.* (2017a). Bending, buckling and buckling of embedded nano-sandwich plates were investigated by Kolahchi (2017) based on refined zigzag theory (RZT), SSDT, first order shear deformation theory (FSDT) and classical plate theory (CPT). Stress, deflection, and frequency analysis of CNT reinforced graded sandwich plate under uniform and linear thermal environment was considered by Mehar *et al.* (2018). A novel and simple higher order shear deformation theory for stability and vibration of functionally graded sandwich plate was investigated by Sekkal *et al.* (2017). Zarei *et al.* (2017) studied dynamic buckling of a sandwich truncated conical shell composed of polymer-carbon nanotubes (CNT)-fiber multiphase nanocomposite layers. Kolahchi *et al.* (2017b) considered wave propagation analysis in a piezoelectric sandwich plate that consists of viscoelastic nanocomposite layers under electro-magnetic field. An exact spectral element method for free vibration analysis of FG plate integrated with piezoelectric layers was performed by Abad and Rouzegar (2017). Optimization of

dynamic buckling for sandwich nanocomposite plates with sensor and actuator layer based on sinusoidal visco-piezoelectricity theories using Grey Wolf algorithm was investigated by Kolahchi *et al.* (2017b). Hajmohammad *et al.* (2017) presented the dynamic buckling of sensor/functionally graded-carbon nanotubes reinforced laminated plates/actuator based on SSDT. Transient response of an active nonlinear sandwich piezo laminated plate was introduced by Oveisi and Nestorović (2016). Sharma *et al.* (2018) analyzed evaluation of vibroacoustic responses of laminated composite sandwich structure using higher-order finite-boundary element model. The global buckling and wrinkling behavior of sandwich plates with anisotropic facesheets was investigated by Vescovini *et al.* (2018) using means of a linearized stability analysis. Katariya *et al.* (2018) evaluated bending and vibration analysis of skew sandwich plate. Smart control and vibration analysis of laminated sandwich truncated conical shells with piezoelectric layers as sensor and actuator were presented by Hajmohammad *et al.* (2018). Katariya and Panda (2019a) investigated numerical evaluation of transient deflection and frequency responses of sandwich shell structure using higher order theory and different mechanical loadings. Frequency and deflection responses of shear deformable skew sandwich curved shell panel was analyzed by Katariya and Panda (2019b).

Due to the lake of research in the field of pizo-sandwich plates according to MR fluid, this work presents the vibration and damping of sandwich plates with MR fluid core contain of piezoelectric layers as sensor and actuator. Furthermore, Halpin-Tsai model is used to determine the material properties of facesheets which are reinforced by GPLs. In addition, the MR fluid core and facesheets are subjected to magnetic field and 3D electric filed, respectively. Motion equations are derived according to SSDT and vibration of the structure is defined by DCM. The effect of different factors such as GPLs distribution, dimensions of structure, electro-magnetic field, damping of structure, viscoelastic environment and boundary conditions of the structure on the vibration and loss factor of the system are considered.

## 2. Formulation

A graphical description of the sandwich plates integrated MR fluid and GPLs piezoelectric facesheets is depicted in Fig. 1. The thickness of sandwich plate varies from  $-h$  to  $h$  and the origin of the Cartesian coordinate system ( $x, y, z$ ) is placed at the mid-plane of the sandwich plate. The geometrical factors of the system are length  $L$ , width  $b$ , actuator thickness, sensor thickness and core thickness. It is assumed that there is not any slipping between the facesheets and MR fluid layers. Parameters of viscoelastic medium are showing by spring and damper. In addition, the MR fluid core and facesheets are subjected to magnetic field and 3D electric filed, respectively. Furthermore, a PD controller is placed in order to receive the sensor signal and after processing it can be applied as actuator input.

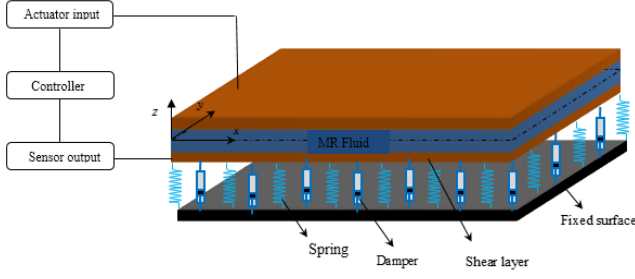


Fig. 1 A graphical description of the sandwich plates integrated MR fluid and GPLs piezoelectric facesheets

## 2.1 Theory of Visco-piezoelectricity

According to piezoelectricity theory, formulation of a piezoelectric material is presented as Kolahchi *et al.* (2016)

$$\begin{bmatrix} \sigma_{xx}^{(P)} \\ \sigma_{yy}^{(P)} \\ \sigma_{zz}^{(P)} \\ \tau_{yz}^{(P)} \\ \tau_{xz}^{(P)} \\ \tau_{xy}^{(P)} \\ D_x^{(P)} \\ D_y^{(P)} \\ D_z^{(P)} \end{bmatrix} = \begin{bmatrix} C_{11}^{(P)} & C_{12}^{(P)} & C_{13}^{(P)} & 0 & 0 & 0 & 0 & 0 & -e_{31}^{(P)} \\ C_{21}^{(P)} & C_{22}^{(P)} & C_{23}^{(P)} & 0 & 0 & 0 & 0 & 0 & -e_{32}^{(P)} \\ C_{31}^{(P)} & C_{32}^{(P)} & C_{33}^{(P)} & 0 & 0 & 0 & 0 & 0 & -e_{33}^{(P)} \\ 0 & 0 & 0 & C_{44}^{(P)} & 0 & 0 & 0 & -e_{24}^{(P)} & 0 \\ 0 & 0 & 0 & 0 & C_{55}^{(P)} & 0 & -e_{15}^{(P)} & 0 & 0 \\ 0 & 0 & 0 & 0 & 0 & C_{66}^{(P)} & 0 & 0 & 0 \\ 0 & 0 & 0 & 0 & e_{15}^{(P)} & 0 & \epsilon_{11}^{(P)} & 0 & 0 \\ 0 & 0 & 0 & e_{23}^{(P)} & 0 & 0 & 0 & \epsilon_{22}^{(P)} & 0 \\ e_{31}^{(P)} & e_{32}^{(P)} & e_{33}^{(P)} & 0 & 0 & 0 & 0 & 0 & \epsilon_{33}^{(P)} \end{bmatrix} \begin{bmatrix} \epsilon_{xx}^{(P)} \\ \epsilon_{yy}^{(P)} \\ \epsilon_{zz}^{(P)} \\ \gamma_{yz}^{(P)} \\ \gamma_{xz}^{(P)} \\ \gamma_{xy}^{(P)} \\ E_x^{(P)} \\ E_y^{(P)} \\ E_z^{(P)} \end{bmatrix} \quad (1)$$

in which  $\epsilon_{kl}$ ,  $\sigma_{ij}$  and  $D_k$  represent the strain, stress and electric displacement, respectively.  $e_{ijk}$ ,  $C_{ij}$  and  $\epsilon_{ij}$  indicate the piezoelectric, elastic stiffness and dielectric coefficients; the superscript (P) is used to show the sensor ((P)=(s)) and the actuator ((P)=(a)) layers;  $E_k$  is the electric field which is expressed according to electric potential ( $\phi$ )

$$E = -\nabla\phi, \quad (2)$$

The electric potential of the sensor and actuator layers are as

$$\phi^{(a)}(x, y, z, t) = \sin\left(\frac{\pi\left(z - \frac{h^{(c)}}{2}\right)}{h^{(a)}}\right) \Phi^{(a)}(x, y, t) + \frac{(z - h^{(c)}/2)V_0}{h^{(a)}} \quad (3)$$

$$\phi^{(s)}(x, y, z, t) = \sin\left(\frac{\pi(-z - h^{(c)}/2)}{h^{(s)}}\right) \Phi^{(s)}(x, y, t), \quad (4)$$

$\Phi^{(P)}$  shows the electric potential in the mid-plane and  $V_0$  expresses the external electric voltage. According to Kelvin-Voigt theory, the elastic stiffness is as Lei *et al.* (2013)

$$C_{ij}^{(P)} = Q_{ij}^{(P)} \left(1 + g \frac{\partial}{\partial t}\right), \quad (5)$$

in which  $g$  indicates the structural damping coefficient and  $Q_{ij}^{(P)}$  can be obtained by Halpin-Tsai model.

## 2.2 Micromechanics model based on Halpin-Tsai

According to the Halpin-Tsai micromechanics model, Young's modulus and Poisson's ratio of the nanocomposite layer are denoted as Yang *et al.* (2017)

$$E_c = \frac{3}{8} \frac{1 + \left(\frac{2L}{t}\right) \left(\frac{\frac{E_{GPL}-1}{E_M} - \frac{E_{GPL}+2L}{E_M}}{\frac{E_{GPL}+2L}{E_M}}\right) V_{GPL}}{1 - \left(\frac{\frac{E_{GPL}-1}{E_M} - \frac{E_{GPL}+2L}{E_M}}{\frac{E_{GPL}+2L}{E_M}}\right) V_{GPL}} E_M + \frac{5}{8} \frac{1 + \left(\frac{2W}{t}\right) \left(\frac{\frac{E_{GPL}/E_M-1}{E_{GPL}/E_M+2W/t} - \frac{E_{GPL}/E_M-1}{E_{GPL}/E_M+2W/t}\right) V_{GPL}}{1 - \left(\frac{E_{GPL}/E_M-1}{E_{GPL}/E_M+2W/t}\right) V_{GPL}} E_M, \quad (6)$$

$$\nu_c = V_{GPL} \nu_{GPL} + (1 - V_{GPL}) \nu_M, \quad (7)$$

$T$ ,  $L$  and  $W$  express the thickness of the GPLs, average length and width.  $E_{GPL}$  and  $E_M$  are the moduli of the GPL and polymer matrix; moreover,  $\nu_M$  and  $\nu_{GPL}$  show the Poisson's ratio of matrix and GPL, respectively.  $V_{GPL}$  is the volume fraction of the GPL nanofillers which is defined as

$$V_{GPL} = \frac{W_{GPL}}{W_{GPL} + (\rho_{GPL}/\rho_M) - (\rho_{GPL}/\rho_M)W_{GPL}}, \quad (8)$$

where  $\rho_{GPL}$  and  $\rho_M$  are the mass densities of GPLs and matrix; in addition,  $W_{GPL}$  is the weight fraction of GPLs. In this study, three distributions of GPLs are considered as follow:

### (1) Linear GPL distribution (Fig. 2(a)):

In this type, the weight fraction of GPLs changes from maximum value to zero as linear.

$$W_{GPL} = w_{GPL} \left(\frac{1}{2} + \frac{z}{h}\right). \quad (9)$$

### (2) Nonlinear GPL distribution (Fig. 2(b)):

In this type, the maximum weight fraction of GPLs is placed at a distances  $s$  from the mid-plane.

$$W_{GPL} = \frac{w_{GPL} z^2}{h^2 s^2 (4s^2 - h^2)} \left[ 4h^2 z^2 - h^4 + \frac{16}{n} s^2 (s^2 - z^2) \right]. \quad (10)$$

$c_1 = c_2/n$  and  $c_2 = w_{GPL}$  in which  $n$  is a positive integer.

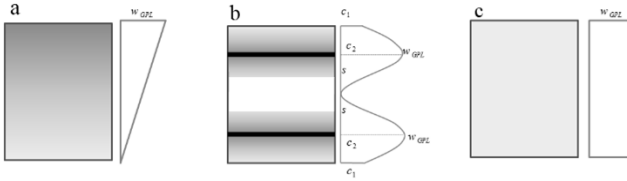


Fig. 2 distribution of GPLs through the thickness of the piezoelectric layers: (a) linear; (b) nonlinear; (c) uniform

(3) Uniform GPL distribution (Fig. 2(c)):

In this type, the weight fraction of GPLs is equal.

$$W_{GPL} = w_{GPL}. \quad (11)$$

In which  $w_{GPL}$  is a unique GPL weight fraction.

### 2.3 SSDT

It is assumed that the transverse displacements of all layers are the same; therefore, SSDT is used to define displacement fields (Kolahchi and Cheraghabak 2017)

$$U^{(i)}(x, y, z, t) = u^{(i)}(x, y, t) - z \frac{\partial w_b}{\partial x} - \left( z - \frac{h}{\pi} \sin \frac{\pi z}{h} \right) \frac{\partial w_s}{\partial x}, \quad (12)$$

$$V^{(i)}(x, y, z, t) = v^{(i)}(x, y, t) - z \frac{\partial w_b}{\partial y} - \left( z - \frac{h}{\pi} \sin \frac{\pi z}{h} \right) \frac{\partial w_s}{\partial y}, \quad (13)$$

$$W(x, y, z, t) = w_b(x, y, t) + w_s(x, y, t), \quad (14)$$

in which  $v$  and  $u$  denote the in-plane displacements,  $w_s$  and  $w_b$  indicate the shear and bending displacements of the mid-plane cross the thickness;  $i$  expresses the sensor (s), actuator (a) and core (c) layers, respectively. Consequently, the strain-displacement formulations is defined as

$$\varepsilon_{xx}^{(s,a)} = \frac{\partial u^{(s,a)}}{\partial x} - z \frac{\partial^2 w_b}{\partial x^2} - f(z) \frac{\partial^2 w_s}{\partial x^2}, \quad (15)$$

$$\varepsilon_{yy}^{(s,a)} = \frac{\partial v^{(s,a)}}{\partial y} - z \frac{\partial^2 w_b}{\partial y^2} - f(z) \frac{\partial^2 w_s}{\partial y^2}, \quad (16)$$

$$\gamma_{xy}^{(s,a)} = \frac{\partial u^{(s,a)}}{\partial y} + \frac{\partial v^{(s,a)}}{\partial x} - 2z \frac{\partial^2 w_b}{\partial y \partial x} - 2f(z) \frac{\partial^2 w_s}{\partial x^2}, \quad (17)$$

$$\gamma_{xz}^{(s,a)} = g(z) \frac{\partial w_s}{\partial x}, \quad (18)$$

$$\gamma_{yz}^{(s,a)} = g(z) \frac{\partial w_s}{\partial y}, \quad (19)$$

where  $f(z) = z - \frac{h}{\pi} \sin \left( \frac{\pi z}{h} \right)$  and  $g(z) = \cos \left( \frac{\pi z}{h} \right)$ .

### 2.4 MR fluid core

The Young's modulus of MR fluid core is very small in comparison with facesheets. Furthermore, the normal stress of this layer can be ignored. Therefore, the shear strain of the MR fluid is expressed as Yeh (2013)

$$\gamma_{xz}^{(c)} = \frac{H}{h^{(c)}} \left( \frac{\partial w_b}{\partial x} + \frac{\partial w_s}{\partial x} + \frac{u_t - u_b}{H} \right), \quad (20)$$

$$\gamma_{yz}^{(c)} = \frac{H}{h^{(c)}} \left( \frac{\partial w_b}{\partial y} + \frac{\partial w_s}{\partial y} + \frac{v_t - v_b}{H} \right), \quad (21)$$

in which  $H = (h^{(t)} + 2h^{(c)} + h^{(b)})/2$ . According to linear viscoelastic theory, the shear stress is defined based on shear strain of MR fluid as

$$\tau_{xz}^{(c)} = G^* \gamma_{xz}^{(c)}, \quad (22)$$

$$\tau_{yz}^{(c)} = G^* \gamma_{yz}^{(c)}, \quad (23)$$

where  $G^*$  is the complex shear modulus of the MR fluid that is

$$G^* = G' + iG'', \quad (24)$$

where  $G'$  and  $G''$  denote the MR fluid storage modulus and loss modulus, respectively and  $\eta = G''/G'$  indicates the loss factor.

### 3. Equations of motion

In this part, in order to calculate the motion equations of the system, energy method and principle of Hamilton are applied.

The potential energy of MR fluid core ( $E_c$ ), the actuator ( $E_a$ ) and sensor ( $E_s$ ) layers are defined as

$$E_a = \frac{1}{2} \int_{A^{(a)}} \int_{\frac{h^{(c)}}{2}}^{\frac{h^{(c)}}{2} + h^{(s)}} \left( \sigma_{xx}^{(a)} \varepsilon_{xx}^{(a)} + \sigma_{yy}^{(a)} \varepsilon_{yy}^{(a)} + \tau_{xz}^{(a)} \gamma_{xz}^{(a)} + \tau_{yz}^{(a)} \gamma_{yz}^{(a)} + \tau_{xy}^{(a)} \gamma_{xy}^{(a)} - D_x^{(a)} E_x^{(a)} - D_y^{(a)} E_y^{(a)} - D_z^{(a)} E_z^{(a)} \right) dz dA, \quad (25)$$

$$E_c = \frac{1}{2} \int_{A^{(c)}} \int_{-h^{(c)}/2}^{h^{(c)}/2} \left( \tau_{xz}^{(c)} \gamma_{xz}^{(c)} + \tau_{yz}^{(c)} \gamma_{yz}^{(c)} \right) dz dA, \quad (26)$$

$$E_s = \frac{1}{2} \int_{A^{(s)}} \int_{-h^{(c)}/2 - h^{(a)}}^{-h^{(c)}/2} \left( \sigma_{xx}^{(s)} \varepsilon_{xx}^{(s)} + \sigma_{yy}^{(s)} \varepsilon_{yy}^{(s)} + \tau_{xz}^{(s)} \gamma_{xz}^{(s)} + \tau_{yz}^{(s)} \gamma_{yz}^{(s)} + \tau_{xy}^{(s)} \gamma_{xy}^{(s)} - D_x^{(s)} E_x^{(s)} - D_y^{(s)} E_y^{(s)} - D_z^{(s)} E_z^{(s)} \right) dz dA, \quad (27)$$

The total potential energy of the system ( $E_{Total} = E_a + E_c + E_s$ ) is as follow

$$E_{Total} = \left[ \frac{1}{2} \int_{A^{(a)}} \left( N_{xx}^{(a)} \frac{\partial u^{(a)}}{\partial x} - M_{xx}^{(a)} \frac{\partial^2 w_b}{\partial x^2} - S_{xx}^{(a)} \frac{\partial^2 w_s}{\partial x^2} + N_{yy}^{(s)} \frac{\partial v^{(a)}}{\partial y} - M_{yy}^{(a)} \frac{\partial^2 w_b}{\partial y^2} - S_{yy}^{(a)} \frac{\partial^2 w_s}{\partial y^2} + N_{xy}^{(a)} \left( \frac{\partial u^{(a)}}{\partial y} + \frac{\partial v^{(a)}}{\partial x} \right) - 2M_{xy}^{(a)} \frac{\partial^2 w_b}{\partial y \partial x} \right) \right] \quad (28)$$

$$\begin{aligned}
& -2S_{xy}^{(a)} \frac{\partial^2 w_s}{\partial x^2} Q_{xz}^{(a)} \left( \frac{\partial w_s}{\partial x} \right) + Q_{yz}^{(a)} \left( \frac{\partial w_s}{\partial y} \right) dA \\
& - \frac{1}{2} \left( \int_{A(a)} \int_{\frac{h^{(c)}}{2}}^{\left(\frac{h^{(c)}}{2} + h^{(a)}\right)} \left[ D_x^{(a)} \left( -\sin \left( \frac{\pi \left( z - \frac{h^{(c)}}{2} \right)}{h^{(a)}} \right) \frac{\partial \Phi^{(a)}}{\partial x} \right) \right. \right. \\
& \left. \left. + D_y^{(a)} \left( -\sin \left( \frac{\pi \left( z - \frac{h^{(c)}}{2} \right)}{h^{(a)}} \right) \frac{\partial \Phi^{(a)}}{\partial y} \right) \right. \right. \\
& \left. \left. + D_z^{(a)} \left( -\frac{\pi}{2} \cos \left( \frac{\pi \left( z - \frac{h^{(c)}}{2} \right)}{h^{(a)}} \right) \Phi^{(a)} - \frac{V_0}{2} \right) \right] dz dA \right) \\
& + \left[ \frac{1}{2} \int_{A(c)} \left( \frac{Q_{xz}^{(c)} H}{h^{(c)}} \left( \frac{\partial w_b}{\partial x} + \frac{\partial w_s}{\partial x} + \frac{u^{(a)} - u^{(s)}}{H} \right) \right. \right. \\
& \left. \left. + \frac{Q_{yz}^{(c)} H}{h^{(c)}} \left( \frac{\partial w_b}{\partial y} + \frac{\partial w_s}{\partial y} + \frac{v^{(a)} - v^{(s)}}{H} \right) \right) dA \right] \\
& + \left[ \frac{1}{2} \int_{A(s)} \left( N_{xx}^{(s)} \frac{\partial u^{(s)}}{\partial x} - M_{xx}^{(s)} \frac{\partial^2 w_b}{\partial x^2} - S_{xx}^{(s)} \frac{\partial^2 w_s}{\partial x^2} \right. \right. \\
& + N_{yy}^{(s)} \frac{\partial v^{(s)}}{\partial y} - M_{yy}^{(s)} \frac{\partial^2 w_b}{\partial y^2} - S_{yy}^{(s)} \frac{\partial^2 w_s}{\partial y^2} \\
& + N_{xy}^{(s)} \left( \frac{\partial u^{(s)}}{\partial y} + \frac{\partial v^{(s)}}{\partial x} \right) - 2M_{xy}^{(s)} \frac{\partial^2 w_b}{\partial y \partial x} - 2S_{xy}^{(s)} \frac{\partial^2 w_s}{\partial x^2} \\
& \left. \left. Q_{xz}^{(s)} \left( \frac{\partial w_s}{\partial x} \right) + Q_{yz}^{(s)} \left( \frac{\partial w_s}{\partial y} \right) \right) dA \right. \\
& - \frac{1}{2} \int_A \int_{-\frac{h^{(c)}}{2}}^{\frac{h^{(c)}}{2}} \left[ D_x^{(s)} \left( -\sin \left( \frac{\pi \left( -z - \frac{h^{(c)}}{2} \right)}{h^{(s)}} \right) \frac{\partial \Phi^{(s)}}{\partial x} \right) \right. \\
& \left. + D_y^{(s)} \left( -\sin \left( \frac{\pi \left( -z - \frac{h^{(c)}}{2} \right)}{h^{(s)}} \right) \frac{\partial \Phi^{(s)}}{\partial y} \right) \right. \\
& \left. + D_z^{(s)} \left( \frac{\pi}{2} \cos \left( \frac{\pi \left( -z - \frac{h^{(c)}}{2} \right)}{h^{(s)}} \right) \Phi^{(s)} \right) \right] dz dA, \quad (28)
\end{aligned}$$

in which the stress resultants are expressed as

$$(N_{xx}^{(a)}, M_{xx}^{(a)}, S_{xx}^{(a)}) = \int_{h^{(c)}/2}^{h^{(c)}/2 + h^{(a)}} \sigma_{xx}^{(a)}(1, z, f(z)) dz, \quad (29)$$

$$(N_{xx}^{(s)}, M_{xx}^{(s)}, S_{xx}^{(s)}) = \int_{-h^{(c)}/2}^{-h^{(c)}/2 - h^{(s)}} \sigma_{xx}^{(s)}(1, z, f(z)) dz, \quad (30)$$

$$(N_{yy}^{(a)}, M_{yy}^{(a)}, S_{yy}^{(a)}) = \int_{h^{(c)}/2}^{h^{(c)}/2 + h^{(a)}} \sigma_{yy}^{(a)}(1, z, f(z)) dz, \quad (31)$$

$$(N_{yy}^{(s)}, M_{yy}^{(s)}, S_{yy}^{(s)}) = \int_{-h^{(c)}/2}^{-h^{(c)}/2 - h^{(s)}} \sigma_{yy}^{(s)}(1, z, f(z)) dz, \quad (32)$$

$$(N_{xy}^{(a)}, M_{xy}^{(a)}, S_{xy}^{(a)}) = \int_{h^{(c)}/2}^{h^{(c)}/2 + h^{(a)}} \sigma_{xx}^{(a)}(1, z, f(z)) dz, \quad (33)$$

$$(N_{xy}^{(s)}, M_{xy}^{(s)}, S_{xy}^{(s)}) = \int_{-h^{(c)}/2}^{-h^{(c)}/2 - h^{(s)}} \sigma_{xx}^{(s)}(1, z, f(z)) dz, \quad (34)$$

$$(Q_{xz}^{(a)}, Q_{yz}^{(a)}) = \int_{h^{(c)}/2}^{h^{(c)}/2 + h^{(a)}} (\tau_{xz}^{(a)}, \tau_{yz}^{(a)}) g(z) dz, \quad (35)$$

$$(Q_{xz}^{(s)}, Q_{yz}^{(s)}) = \int_{-h^{(c)}/2}^{-h^{(c)}/2 - h^{(s)}} (\tau_{xz}^{(s)}, \tau_{yz}^{(s)}) g(z) dz, \quad (36)$$

$$(Q_{xz}^{(c)}, Q_{yz}^{(c)}) = \int_{-h^{(c)}/2}^{h^{(c)}/2} (\tau_{xz}^{(c)}, \tau_{yz}^{(c)}) dz, \quad (37)$$

The kinetic energy of MR fluid core ( $K_c$ ), the actuator ( $K_a$ ) and sensor ( $K_s$ ) layers are as

$$\begin{aligned}
K_a = & \frac{\rho^{(a)}}{2} \int_{A(a)} \int_{\frac{h^{(c)}}{2}}^{\frac{h^{(c)}}{2} + h^{(a)}} \left[ \left( \frac{\partial u^{(a)}}{\partial t} \right)^2 + z^2 \left( \frac{\partial^2 w_b}{\partial x \partial t} \right)^2 \right. \\
& + f(z)^2 \left( \frac{\partial^2 w_s}{\partial x \partial t} \right)^2 - 2z \frac{\partial u^{(a)}}{\partial t} \frac{\partial^2 w_b}{\partial x \partial t} \\
& - 2f(z) \frac{\partial u^{(a)}}{\partial t} \frac{\partial^2 w_s}{\partial x \partial t} - 2zf(z) \frac{\partial^2 w_b}{\partial x \partial t} \frac{\partial^2 w_s}{\partial x \partial t} \\
& + \left( \frac{\partial v^{(a)}}{\partial t} \right)^2 + z^2 \left( \frac{\partial^2 w_b}{\partial y \partial t} \right)^2 + f(z)^2 \left( \frac{\partial^2 w_s}{\partial y \partial t} \right)^2 \\
& - 2z \frac{\partial v^{(a)}}{\partial t} \frac{\partial^2 w_b}{\partial y \partial t} - 2f(z) \frac{\partial v^{(a)}}{\partial t} \frac{\partial^2 w_s}{\partial y \partial t} \\
& - 2zf(z) \frac{\partial^2 w_b}{\partial y \partial t} \frac{\partial^2 w_s}{\partial y \partial t} + \left( \frac{\partial w_b}{\partial t} \right)^2 \\
& \left. + \left( \frac{\partial w_s}{\partial t} \right)^2 + 2 \frac{\partial w_b}{\partial t} \frac{\partial w_s}{\partial t} \right] dz dA, \quad (38)
\end{aligned}$$

$$\begin{aligned}
K_c = & \frac{\rho^{(c)}}{2} \int_{A(c)} \int_{-\frac{h^{(c)}}{2}}^{\frac{h^{(c)}}{2}} \left[ \left( \frac{\partial w_b}{\partial t} \right)^2 + \left( \frac{\partial w_s}{\partial t} \right)^2 \right. \\
& \left. + z^2 \left( \frac{\partial \gamma_{xz}^{(c)}}{\partial t} \right)^2 + z^2 \left( \frac{\partial \gamma_{yz}^{(c)}}{\partial t} \right)^2 \right] dz dA, \quad (39)
\end{aligned}$$

$$\begin{aligned}
K_s = & \frac{\rho^{(s)}}{2} \int_{A(s)} \int_{-\frac{h^{(c)}}{2} - h^{(s)}}^{-\frac{h^{(c)}}{2}} \left[ \left( \frac{\partial u^{(s)}}{\partial t} \right)^2 + z^2 \left( \frac{\partial^2 w_b}{\partial x \partial t} \right)^2 \right. \\
& + f(z)^2 \left( \frac{\partial^2 w_s}{\partial x \partial t} \right)^2 - 2z \frac{\partial u^{(s)}}{\partial t} \frac{\partial^2 w_b}{\partial x \partial t} \\
& - 2f(z) \frac{\partial u^{(s)}}{\partial t} \frac{\partial^2 w_s}{\partial x \partial t} - 2zf(z) \frac{\partial^2 w_b}{\partial x \partial t} \frac{\partial^2 w_s}{\partial x \partial t} \\
& + \left( \frac{\partial v^{(s)}}{\partial t} \right)^2 + z^2 \left( \frac{\partial^2 w_b}{\partial y \partial t} \right)^2 + f(z)^2 \left( \frac{\partial^2 w_s}{\partial y \partial t} \right)^2 \\
& - 2z \frac{\partial v^{(s)}}{\partial t} \frac{\partial^2 w_b}{\partial y \partial t} - 2f(z) \frac{\partial v^{(s)}}{\partial t} \frac{\partial^2 w_s}{\partial y \partial t} \\
& - 2zf(z) \frac{\partial^2 w_b}{\partial y \partial t} \frac{\partial^2 w_s}{\partial y \partial t} + \left( \frac{\partial w_b}{\partial t} \right)^2 \\
& \left. + \left( \frac{\partial w_s}{\partial t} \right)^2 + 2 \frac{\partial w_b}{\partial t} \frac{\partial w_s}{\partial t} \right] dz dA, \quad (40)
\end{aligned}$$

The total kinetic energy of system ( $K_{Total} = K_a + K_c + K_s$ ) is defined as

$$\begin{aligned}
K_{Total} = & \frac{1}{2} \int_{A(a)} \left[ I_0^{(a)} \left\{ \left( \frac{\partial u^{(a)}}{\partial t} \right)^2 + \left( \frac{\partial v^{(a)}}{\partial t} \right)^2 \right. \right. \\
& \left. \left. + \left( \frac{\partial w_b}{\partial t} + \frac{\partial w_s}{\partial t} \right)^2 \right\} \right. \\
& \left. + I_1^{(a)} \left\{ -2 \frac{\partial u^{(a)}}{\partial t} \frac{\partial^2 w_b}{\partial x \partial t} - 2 \frac{\partial v^{(a)}}{\partial t} \frac{\partial^2 w_b}{\partial y \partial t} \right\} \right] dz dA, \quad (41)
\end{aligned}$$

$$\begin{aligned}
& +I_2^{(a)} \left\{ \left( \frac{\partial^2 w_b}{\partial x \partial t} \right)^2 + \left( \frac{\partial^2 w_b}{\partial y \partial t} \right)^2 \right\} \\
& +I_3^{(a)} \left\{ -2 \frac{\partial u^{(a)}}{\partial t} \frac{\partial^2 w_s}{\partial x \partial t} - 2 \frac{\partial v^{(a)}}{\partial t} \frac{\partial^2 w_s}{\partial y \partial t} \right\} \\
& +I_4^{(a)} \left\{ \left( \frac{\partial^2 w_s}{\partial x \partial t} \right)^2 + \left( \frac{\partial^2 w_s}{\partial y \partial t} \right)^2 \right\} \\
& +I_5^{(a)} \left\{ -2 \frac{\partial^2 w_b}{\partial x \partial t} \frac{\partial^2 w_s}{\partial x \partial t} - 2 \frac{\partial^2 w_b}{\partial y \partial t} \frac{\partial^2 w_s}{\partial y \partial t} \right\} \Big] dz dA \\
& + \frac{1}{2} \int_{A^{(c)}} \left[ I_0^{(c)} \left\{ \left( \frac{\partial w_b}{\partial t} + \frac{\partial w_s}{\partial t} \right)^2 \right. \right. \\
& + I_2^{(c)} \left( \frac{H}{h^{(c)}} \right)^2 \left\{ \left( \frac{\partial^2 w_b}{\partial x \partial t} \right)^2 + \left( \frac{\partial^2 w_s}{\partial x \partial t} \right)^2 \right. \\
& + \left( \frac{\partial u^{(a)}}{H \partial t} \right)^2 + \left( \frac{\partial u^{(s)}}{H \partial t} \right)^2 + 2 \frac{\partial^2 w_b}{\partial x \partial t} \frac{\partial^2 w_s}{\partial x \partial t} \\
& + 2 \frac{\partial^2 w_b}{\partial x \partial t} \frac{\partial u^{(a)}}{H \partial t} - 2 \frac{\partial^2 w_b}{\partial x \partial t} \frac{\partial u^{(s)}}{H \partial t} \\
& + 2 \frac{\partial^2 w_s}{\partial x \partial t} \frac{\partial u^{(a)}}{H \partial t} - 2 \frac{\partial^2 w_s}{\partial x \partial t} \frac{\partial u^{(s)}}{H \partial t} - 2 \frac{\partial u^{(a)}}{H \partial t} \frac{\partial u^{(s)}}{H \partial t} \\
& + \left( \frac{\partial^2 w_b}{\partial y \partial t} \right)^2 + \left( \frac{\partial^2 w_s}{\partial y \partial t} \right)^2 + \left( \frac{\partial v^{(a)}}{H \partial t} \right)^2 \\
& + \left( \frac{\partial v^{(s)}}{H \partial t} \right)^2 + 2 \frac{\partial^2 w_b}{\partial y \partial t} \frac{\partial^2 w_s}{\partial y \partial t} + 2 \frac{\partial^2 w_b}{\partial y \partial t} \frac{\partial v^{(a)}}{H \partial t} \\
& - 2 \frac{\partial^2 w_b}{\partial y \partial t} \frac{\partial v^{(s)}}{H \partial t} + 2 \frac{\partial^2 w_s}{\partial y \partial t} \frac{\partial v^{(a)}}{H \partial t} \\
& \left. \left. - 2 \frac{\partial^2 w_s}{\partial y \partial t} \frac{\partial v^{(s)}}{H \partial t} - 2 \frac{\partial v^{(a)}}{H \partial t} \frac{\partial v^{(s)}}{H \partial t} \right\} \right] dz dA \\
& + \frac{1}{2} \int_{A^{(a)}} \left[ I_0^{(s)} \left\{ \left( \frac{\partial u^{(s)}}{\partial t} \right)^2 + \left( \frac{\partial v^{(s)}}{\partial t} \right)^2 \right. \right. \\
& + \left( \frac{\partial w_b}{\partial t} \right)^2 + \left( \frac{\partial w_s}{\partial t} \right)^2 \Big\} \\
& + I_1^{(s)} \left\{ -2 \frac{\partial u^{(s)}}{\partial t} \frac{\partial^2 w_b}{\partial x \partial t} - 2 \frac{\partial v^{(s)}}{\partial t} \frac{\partial^2 w_b}{\partial y \partial t} \right\} \\
& + I_2^{(s)} \left\{ \left( \frac{\partial^2 w_b}{\partial x \partial t} \right)^2 + \left( \frac{\partial^2 w_b}{\partial y \partial t} \right)^2 \right\} \\
& + I_3^{(s)} \left\{ -2 \frac{\partial u^{(s)}}{\partial t} \frac{\partial^2 w_s}{\partial x \partial t} - 2 \frac{\partial v^{(s)}}{\partial t} \frac{\partial^2 w_s}{\partial y \partial t} \right\} \\
& + I_4^{(s)} \left\{ \left( \frac{\partial^2 w_s}{\partial x \partial t} \right)^2 + \left( \frac{\partial^2 w_s}{\partial y \partial t} \right)^2 \right\} \\
& + I_5^{(s)} \left\{ -2 \frac{\partial^2 w_b}{\partial x \partial t} \frac{\partial^2 w_s}{\partial x \partial t} - 2 \frac{\partial^2 w_b}{\partial y \partial t} \frac{\partial^2 w_s}{\partial y \partial t} \right\} \Big] dz dA,
\end{aligned} \quad (41)$$

in which the moments of inertia could be given as

$$\begin{aligned}
& (I_0^{(a)}, I_1^{(a)}, I_2^{(a)}, I_3^{(a)}, I_4^{(a)}, I_5^{(a)}) \\
& = \int_{h^{(c)}/2}^{h^{(c)}/2+h^{(a)}} \rho^{(a)}(1, z, z^2, f(z), f(z)^2, zf(z)) dz, \quad (42)
\end{aligned}$$

$$(I_0^{(c)}, I_2^{(c)}) = \int_{-h^{(c)}/2}^{h^{(c)}/2} \rho^{(c)}(1, z^2) dz, \quad (43)$$

$$\begin{aligned}
& (I_0^{(s)}, I_1^{(s)}, I_2^{(s)}, I_3^{(s)}, I_4^{(s)}, I_5^{(s)}) \\
& = \int_{-h^{(c)}/2}^{-h^{(c)}/2-h^{(s)}} \rho^{(s)}(1, z, z^2, f(z), f(z)^2, zf(z)) dz. \quad (44)
\end{aligned}$$

The external force of the orthotropic visco-Pasternak is (Kolahchi *et al.* 2016, Yaylaci and Birinci 2013)

$$\begin{aligned}
q_v = & k_{1w} u_3 + k_{2w} u_3^3 + c_d \dot{u}_3 \\
& - k_{g\xi} \left( \cos^2 \theta \frac{\partial^2 u_3}{\partial x^2} + 2 \cos \theta \sin \theta \frac{\partial^2 u_3}{\partial x \partial y} \right. \\
& + \sin^2 \theta \frac{\partial^2 u_3}{\partial y^2} \Big) - k_{g\zeta} \left( \sin^2 \theta \frac{\partial^2 u_3}{\partial x^2} \right. \\
& \left. - 2 \sin \theta \cos \theta \frac{\partial^2 u_3}{\partial x \partial y} + \cos^2 \theta \frac{\partial^2 u_3}{\partial y^2} \right), \quad (45)
\end{aligned}$$

in which angle  $\theta$  indicates the local  $\xi$  of the orthotropic foundation based on the global  $x$ -axis of the system. Also  $c_d, k_{1w}, k_{2w}, k_{g\xi}$  and  $k_{g\zeta}$  indicate damping, normal spring, nonlinear spring,  $\xi$ -shear and  $\zeta$ -shear constants, respectively. Therefore, the work of the viscoelastic medium force is expressed as

$$V_e = - \int_{A^{(s)}} q_v dA. \quad (46)$$

In order to derive motion equations of system, Hamilton's principle is used as

$$\begin{aligned}
\delta u^{(a)}: & \frac{\partial N_{xx}^{(a)}}{\partial x} + \frac{\partial N_{xy}^{(a)}}{\partial y} - \frac{Q_{xz}^{(c)}}{h^{(c)}} \\
& = I_0^{(a)} \frac{\partial^2 u^{(a)}}{\partial t^2} - I_1^{(a)} \frac{\partial^3 w_b}{\partial x \partial t^2} - I_3^{(a)} \frac{\partial^3 w_s}{\partial x \partial t^2} \\
& + I_2^{(c)} \left( \frac{H}{h^{(c)}} \right)^2 \left( \frac{\partial^3 w_b}{H \partial x \partial t^2} + \frac{\partial^3 w_s}{H \partial x \partial t^2} \right. \\
& \left. + \frac{\partial^2 u^{(a)}}{H^2 \partial t^2} - \frac{\partial^2 u^{(s)}}{H^2 \partial t^2} \right), \quad (47)
\end{aligned}$$

$$\begin{aligned}
\delta u^{(s)}: & \frac{\partial N_{xx}^{(s)}}{\partial x} + \frac{\partial N_{xy}^{(s)}}{\partial y} + \frac{Q_{xz}^{(c)}}{h^{(c)}} \\
& = I_0^{(a)} \frac{\partial^2 u^{(s)}}{\partial t^2} - I_1^{(s)} \frac{\partial^3 w_b}{\partial x \partial t^2} - I_3^{(s)} \frac{\partial^3 w_s}{\partial x \partial t^2} \\
& - I_2^{(c)} \left( \frac{H}{h^{(c)}} \right)^2 \left( \frac{\partial^3 w_b}{H \partial x \partial t^2} + \frac{\partial^3 w_s}{H \partial x \partial t^2} \right. \\
& \left. + \frac{\partial^2 u^{(a)}}{H^2 \partial t^2} - \frac{\partial^2 u^{(s)}}{H^2 \partial t^2} \right), \quad (48)
\end{aligned}$$

$$\begin{aligned}
\delta v^{(a)}: & \frac{\partial N_{yy}^{(a)}}{\partial y} + \frac{\partial N_{xy}^{(a)}}{\partial x} - \frac{Q_{yz}^{(c)}}{h^{(c)}} \\
& = I_0^{(a)} \frac{\partial^2 v}{\partial t^2} - I_1^{(a)} \frac{\partial^3 w_b}{\partial y \partial t^2} - I_3^{(a)} \frac{\partial^3 w_s}{\partial y \partial t^2} \\
& + I_2^{(c)} \left( \frac{H}{h^{(c)}} \right)^2 \left( \frac{\partial^3 w_b}{H \partial y \partial t^2} + \frac{\partial^3 w_s}{H \partial y \partial t^2} \right. \\
& \left. + \frac{\partial^2 v^{(a)}}{H^2 \partial t^2} - \frac{\partial^2 v^{(s)}}{H^2 \partial t^2} \right), \quad (49)
\end{aligned}$$

$$\begin{aligned}
\delta v^{(s)}: & \frac{\partial N_{yy}^{(s)}}{\partial y} + \frac{\partial N_{xy}^{(s)}}{\partial x} + \frac{Q_{yz}^{(c)}}{h^{(c)}} \\
& = I_0^{(s)} \frac{\partial^2 v}{\partial t^2} - I_1^{(s)} \frac{\partial^3 w_b}{\partial y \partial t^2} - I_3^{(s)} \frac{\partial^3 w_s}{\partial y \partial t^2} \quad (50)
\end{aligned}$$

$$-I_2^{(c)} \left( \frac{H}{h^{(c)}} \right)^2 \left( \frac{\partial^3 w_b}{H \partial y \partial t^2} + \frac{\partial^3 w_s}{H \partial y \partial t^2} + \frac{\partial^2 v^{(a)}}{H^2 \partial t^2} - \frac{\partial^2 v^{(s)}}{H^2 \partial t^2} \right), \quad (50)$$

$$\begin{aligned} \delta w_b: & \frac{\partial^2}{\partial x^2} (M_{xx}^{(a)} + M_{xx}^{(s)}) + \frac{\partial^2}{\partial y^2} (M_{yy}^{(a)} + M_{yy}^{(s)}) \\ & + 2 \frac{\partial^2}{\partial y \partial x} (M_{xy}^{(a)} + M_{xy}^{(s)}) \\ & + \frac{H}{h^{(c)}} \frac{\partial Q_{xz}^{(c)}}{\partial x} + \frac{H}{h^{(c)}} \frac{\partial Q_{yz}^{(c)}}{\partial y} \\ & + N_{xe} \left( \frac{\partial^2 w_b}{\partial x^2} + \frac{\partial^2 w_s}{\partial x^2} \right) \\ & + N_{ye} \left( \frac{\partial^2 w_b}{\partial y^2} + \frac{\partial^2 w_s}{\partial y^2} \right) - q_v \\ & - \left( I_2^{(a)} + I_2^{(s)} + I_2^{(c)} \left( \frac{H}{h^{(c)}} \right)^2 \right) \\ & \left( \frac{\partial^4 w_b}{\partial x^2 \partial t^2} + \frac{\partial^4 w_b}{\partial y^2 \partial t^2} \right) \\ & + \left( I_1^{(a)} - I_2^{(c)} \frac{H}{(h^{(c)})^2} \right) \left( \frac{\partial^3 u^{(a)}}{\partial x \partial t^2} + \frac{\partial^3 v^{(a)}}{\partial y \partial t^2} \right) \\ & + \left( I_1^{(s)} + I_2^{(c)} \frac{H}{(h^{(c)})^2} \right) \left( \frac{\partial^3 u^{(s)}}{\partial x \partial t^2} + \frac{\partial^3 v^{(s)}}{\partial y \partial t^2} \right) \\ & - (I_0^{(a)} + I_0^{(s)} + I_0^{(c)}) \left( \frac{\partial^2 w_b}{\partial t^2} + \frac{\partial^2 w_s}{\partial t^2} \right) \\ & + \left( I_5^{(a)} + I_5^{(s)} - I_2^{(c)} \left( \frac{H}{h^{(c)}} \right)^2 \right) \\ & \left( \frac{\partial^4 w_s}{\partial x^2 \partial t^2} + \frac{\partial^4 w_s}{\partial y^2 \partial t^2} \right), \end{aligned} \quad (51)$$

$$\begin{aligned} \delta w_s: & \frac{\partial^2}{\partial x^2} (S_{xx}^{(a)} + S_{xx}^{(s)}) + \frac{\partial^2}{\partial y^2} (S_{yy}^{(a)} + S_{yy}^{(s)}) \\ & + 2 \frac{\partial^2}{\partial y \partial x} (S_{xy}^{(a)} + S_{xy}^{(s)}) - (Q_{xz}^{(a)} + S_{xz}^{(s)}) \\ & - (Q_{yz}^{(a)} + S_{yz}^{(s)}) + \frac{H}{h^{(c)}} \frac{\partial Q_{xz}^{(c)}}{\partial x} + \frac{H}{h^{(c)}} \frac{\partial Q_{yz}^{(c)}}{\partial y} \\ & + N_{xe} \left( \frac{\partial^2 w_b}{\partial x^2} + \frac{\partial^2 w_s}{\partial x^2} \right) + N_{ye} \left( \frac{\partial^2 w_b}{\partial y^2} + \frac{\partial^2 w_s}{\partial y^2} \right) \\ & - q_v = (I_0^{(a)} + I_0^{(s)} + I_0^{(c)}) \left( \frac{\partial^2 w_b}{\partial t^2} + \frac{\partial^2 w_s}{\partial t^2} \right) \\ & + \left( I_5^{(a)} + I_5^{(s)} + I_2^{(c)} \left( \frac{H}{h^{(c)}} \right)^2 \right) \\ & \left( \frac{\partial^4 w_b}{\partial x^2 \partial t^2} + \frac{\partial^4 w_b}{\partial y^2 \partial t^2} \right) \\ & - \left( I_4^{(a)} + I_4^{(s)} + I_2^{(c)} \left( \frac{H}{h^{(c)}} \right)^2 \right) \\ & \left( \frac{\partial^4 w_s}{\partial x^2 \partial t^2} + \frac{\partial^4 w_s}{\partial y^2 \partial t^2} \right) \\ & + \left( I_3^{(a)} - I_2^{(c)} \frac{H}{(h^{(c)})^2} \right) \left( \frac{\partial^3 u^{(a)}}{\partial x \partial t^2} + \frac{\partial^3 v^{(a)}}{\partial y \partial t^2} \right) \\ & + \left( I_3^{(s)} + I_2^{(c)} \frac{H}{(h^{(c)})^2} \right) \left( \frac{\partial^3 u^{(s)}}{\partial x \partial t^2} + \frac{\partial^3 v^{(s)}}{\partial y \partial t^2} \right), \end{aligned} \quad (52)$$

$$\begin{aligned} \delta \Phi^{(a)}: & \int_{\frac{h^{(c)}}{2}}^{\left(\frac{h^{(c)}}{2} + h^{(a)}\right)} \left[ \left( \sin \left( \frac{\pi \left( z - \frac{h^{(c)}}{2} \right)}{h^{(a)}} \right) \frac{\partial D_x^{(a)}}{\partial x} \right) \right. \\ & + \left( \sin \left( \frac{\pi \left( z - \frac{h^{(c)}}{2} \right)}{h^{(a)}} \right) \frac{\partial D_y^{(a)}}{\partial y} \right) \\ & \left. - \left( \frac{\pi}{2} \cos \left( \frac{\pi \left( z - \frac{h^{(c)}}{2} \right)}{h^{(a)}} \right) D_z^{(a)} \right) \right] dz, \end{aligned} \quad (53)$$

$$\begin{aligned} \delta \Phi^{(s)}: & \int_{-\left(\frac{h^{(c)}}{2h^{(s)}}\right)}^{-\frac{h^{(c)}}{2}} \left[ \left( \sin \left( \frac{\pi \left( -z - \frac{h^{(c)}}{2} \right)}{h^{(s)}} \right) \frac{\partial D_x^{(s)}}{\partial x} \right) \right. \\ & + \left( \sin \left( \frac{\pi \left( -z - \frac{h^{(c)}}{2} \right)}{h^{(s)}} \right) \frac{\partial D_y^{(s)}}{\partial y} \right) \\ & \left. + \left( \frac{\pi}{2} \cos \left( \frac{\pi \left( -z - \frac{h^{(c)}}{2} \right)}{h^{(s)}} \right) D_z^{(s)} \right) \right] dz. \end{aligned} \quad (54)$$

in which are the combination of electric forces ( $N_{xe}$ ) and mechanical forces ( $N_{ye}$ ) are defined as

$$N_x^M = 0; N_x^E = 2e_{31}^{(a)} h^{(a)} V_0, \quad (55)$$

$$N_y^M = 0; N_y^E = 2e_{32}^{(a)} h^{(a)} V_0, \quad (56)$$

The stress resultants can be obtained by substituting Eqs. (15)-(19) into Eqs. (29)-(37). These parameters are evaluated in Appendix A.

In this research, three different boundary conditions are assumed. (clamped supported, simply supported in two edges and clamped in two another edges and simply supported)

## 4. Solving and control method

### 4.1 DCM

In order to calculate the vibration of system a numerical method which is called DCM is applied in this study. DCM denotes a calculus operator ( $\Re$ ) value of the function ( $f(x, y)$ ) at a discrete point in the solution domain. For a two-dimensional problem, the cubature approximation at the  $i^{\text{th}}$  discrete point is as (Kolahchi *et al.* 2016, Öner *et al.* 2014, Birinci *et al.* 2015)

$$\Re f(x, y)_i \approx \sum_{j=1}^N C_{ij} f(x_j, y_j), \quad (57)$$

in which  $N$  and  $C_{ij}$  are the cubature total number of grid points and weighting coefficients, respectively. The computation of the weighting coefficients are defined as

$$\Re \{x^{\nu-\mu} y^{\mu}\}_i = \sum_{j=1}^N C_{ij} f(x_j^{\nu-\mu} y_j^{\mu}), \quad (58)$$

$$\begin{aligned}\mu &= 0, 1, 2, \dots, \nu, \\ \nu &= 0, 1, 2, \dots, N-1, \\ i &= 1, 2, \dots, N.\end{aligned}\quad (58)$$

in matrix form can be shown as

$$\begin{bmatrix} x_j^{\nu-\mu} y_j^\mu \\ \vdots \\ C_{in} \end{bmatrix} = [\Re\{x^{\nu-\mu} y^\mu\}_i]. \quad (59)$$

By using DCM, equations of motion may be gain as

$$\begin{aligned} \underbrace{\begin{bmatrix} M_{bb} & M_{bd} \\ M_{db} & M_{dd} \end{bmatrix}}_{M^*} \underbrace{\begin{bmatrix} \ddot{Y}_b \\ \ddot{Y}_d \end{bmatrix}}_{\dot{Y}} + \underbrace{\begin{bmatrix} C_{bb} & C_{bd} \\ C_{db} & C_{dd} \end{bmatrix}}_{C^*} \underbrace{\begin{bmatrix} \dot{Y}_b \\ \dot{Y}_d \end{bmatrix}}_{\dot{Y}} \\ + \underbrace{\begin{bmatrix} K_{bb} & K_{bd} \\ K_{db} & K_{dd} \end{bmatrix}}_{K^*} \underbrace{\begin{bmatrix} Y_b \\ Y_d \end{bmatrix}}_{Y} = \begin{bmatrix} 0 \\ 0 \end{bmatrix}, \end{aligned} \quad (60)$$

where  $[M]$ ,  $[C]$ ,  $[K]$ ,  $[K^G]$  and  $\{Y\}$  indicate the mass matrix, damp matrix, stiffness matrix, geometric matrix and the displacement vector, respectively.

#### 4.2 PD controller

A proportional-derivative (PD) controller is used (Yang et al. 2017) in order to control the dynamic and vibration responses of the structure. Hence, the electric potential of the actuator layer can be defined as follows

$$\phi^{(a)} = G_d \phi^{(s)} + G_v \dot{\phi}^{(s)}. \quad (61)$$

where  $G_d$  and  $G_v$  denote the proportional and derivative control coefficients, respectively.

#### 4.3 Vibration and damping analysis

Based on eigenvalue problem, Eq. (60) can be solved for obtaining the frequency and damping of the sandwich structure from the following relations

$$\omega = \sqrt{\operatorname{Re}(\lambda)}, \quad (62)$$

$$\eta = \frac{\operatorname{Im}(\lambda)}{\operatorname{Re}(\lambda)}. \quad (63)$$

where  $\lambda$  is the eigenvalue.

### 5. Results and discussion

In this study, some of geometric parameters are used as

$$\begin{aligned} a/b &= 2, & L/h &= 5, \\ h^{(a)}/h^{(s)} &= 1, & h^{(c)}/h^{(a)} &= 0.5 \end{aligned} \quad (64)$$

The density of MR fluid  $\rho^{(c)} = 3500 \text{ Kg/m}^3$  and the storage and loss modulus as Yeh (2013)

$$G' = -3.3691B^2 + 4997.5B + 873000, \quad (65)$$

$$G'' = -0.9B^2 + 812.4B + 185500. \quad (66)$$

Properties of facesheets are as

$$\begin{aligned} E_M &= 129 \text{ GPa}, & \nu_M &= 0.34, \\ \rho^{(P)} &= 5610 \text{ kg/m}^3, & e_{31}^{(P)} &= e_{32}^{(P)} = -0.51 \text{ C/m}^2, \\ \epsilon_{11}^{(P)} &= \epsilon_{22}^{(P)} = 77.7 \text{ nF/m}^2, & \epsilon_{33}^{(P)} &= 89.1 \text{ nF/m}^2 \end{aligned} \quad (67)$$

Moreover, the characteristics of GPLs are as follow (Yang et al. 2017)

$$\begin{aligned} L &= 2.5 \mu\text{m}, & W &= 1.5 \mu\text{m}, & t &= 1.5 \text{ nm}, \\ v_{GPL} &= 0.006, & E_{GPL} &= 1.01 \text{ TPa}, \\ \rho_{GPL} &= 1060 \text{ kg/m}^3, & w_{GPL} &= 1\% \end{aligned} \quad (68)$$

To validate this work, the results of this study are compared with Lall et al. (1987) and Yeh (2013). Table 1 indicates the frequency and loss factor for first four vibrational modes. It can be understood that, the results of this study are close to the results of Lall et al. (1987) and Yeh (2013).

Moreover, the other comparison has been done with Yeh (2013) and Lall et al. (1987).

For different boundary conditions, the frequency of the system is depicted in terms of the DCM grid point numbers. It is obvious that for  $N = 113$  the results become converge. Thus, for analyzing the behavior of structure number of grid points is chosen 113.

Table 1 Frequency and loss factor

Mode	Lall et al. (1987)		Yeh (2013)		Present work	
	$\omega$ (Hz)	$\xi$	$\omega$ (Hz)	$\xi$	$\omega$ (Hz)	$\xi$
1	59.05	0.206	58.69	0.201	58.88	0.202
2	113.67	0.213	113.75	0.211	113.65	0.212
3	128.89	0.207	129.16	0.208	129.18	0.208
4	175.76	0.188	175.46	0.189	175.55	0.177
5	193.67	0.179	193.79	0.183	193.85	0.184

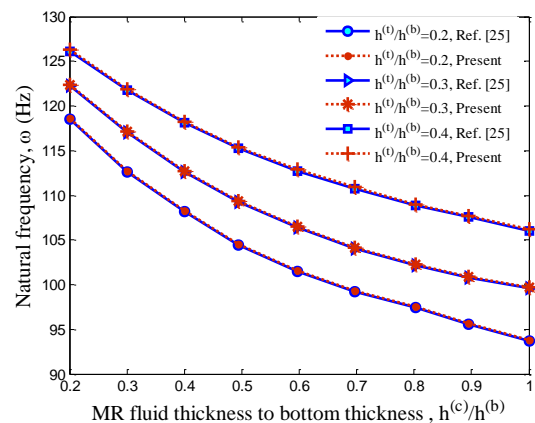


Fig. 3 Comparisons of this work with Yeh (Lall et al. 1987)



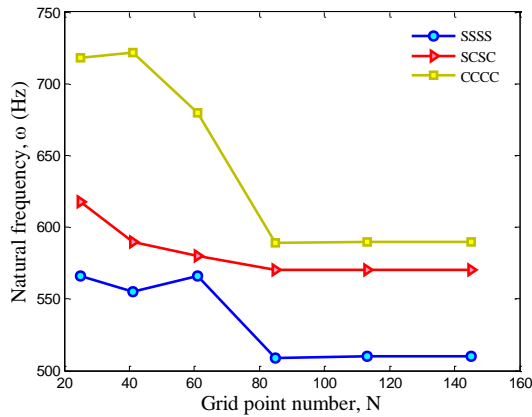
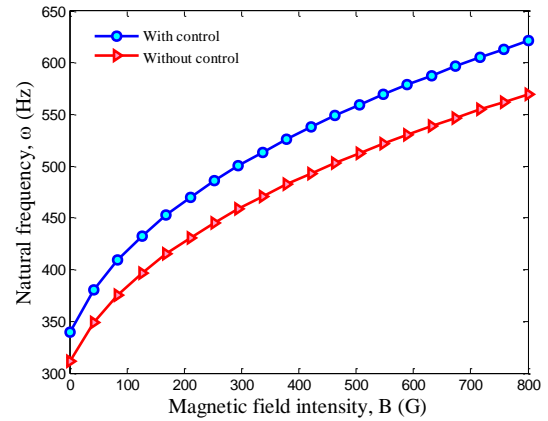
Fig. 4 Comparisons of this study with Yeh (Xu *et al.* 2018)

Fig. 7 PD controller effect on the vibration of the system

### 5.1 Vibration and damping analysis

Natural frequency and modal loss factor versus magnetic field intensity are analyzed in this section. It is mention that the results are represented in the existence of the PD controller. The effect of different boundary condition on the vibration and modal loss factor of the sandwich structure are shown in Figs. 5 and 6. Three different boundary conditions are analyzed, including four

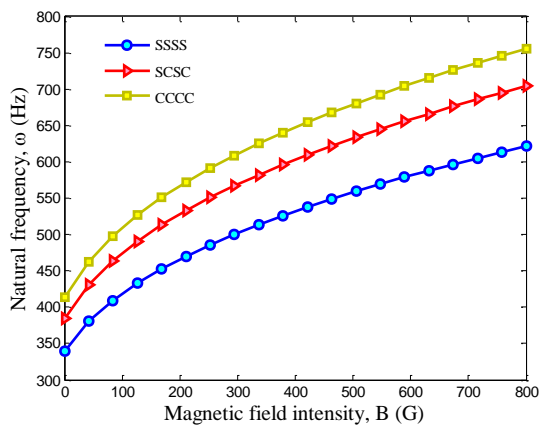


Fig. 5 Boundary condition effect on the vibration of the system

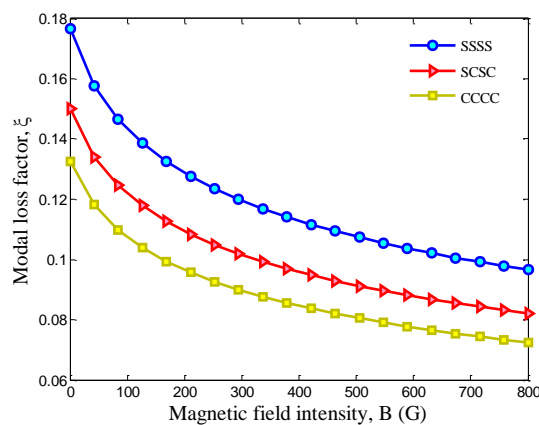


Fig. 6 Boundary condition effect on the modal loss factor

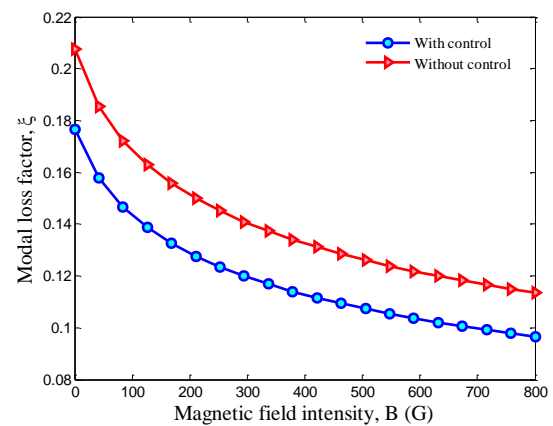


Fig. 8 PD controller effect on the loss factor of the system

edges simply-supported (SSSS), four edges clamped (CCCC) and two edges simply-supported and two edges clamped (SCSC). It is understood that the vibration of the structure with CCCC boundary condition is higher than two other boundary conditions. Indeed, this means that the bending rigidity of sandwich plate with CCCC boundary is higher than others. Moreover, the variation of the modal loss factor is vice versa of the vibration; therefore, the modal loss factor of the structure with CCCC boundary condition is lower than two other boundary conditions.

In Figs. 7 and 8, the vibration and loss factor of the sandwich system without existence of controller are happened at lower and higher magnitude, respectively. Thus, the DIR of the structure with PD controller will be improved and the vibration moves to higher frequencies and loss factor shifts to lower value.

The effects of weight percent ( $w_{GPL}$ ) and distribution types of GPLs on the vibration and loss factor of the structure are depicted in Figs. 9, 10, 11 and 12. It is apparent that by increasing the weight percent of GPLs, the vibration and loss factor are moved to upward and downward, respectively. This is reasonable, because increasing the weight percent of GPLs causes more bending rigidity of the structure.

Figs. 11 and 12 indicate that for the nonlinear and linear distributions of the GPLs, the vibration of the system occurs

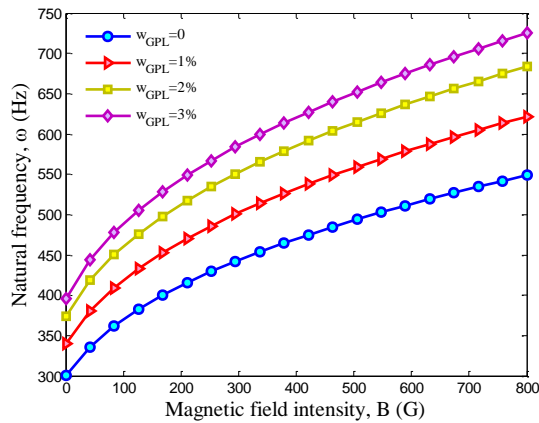


Fig. 9 Weight percent effect of the GPLs on the vibration

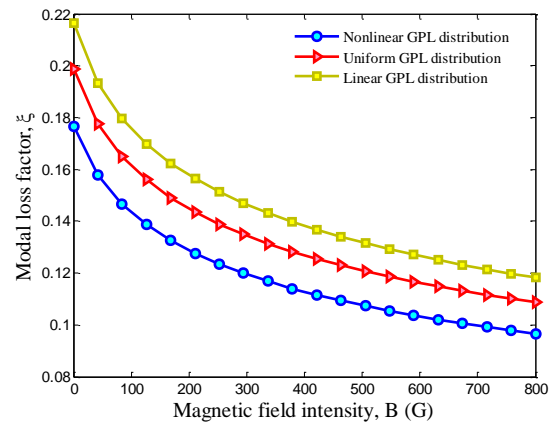


Fig. 12 distribution of GPLs loss factor of the plate

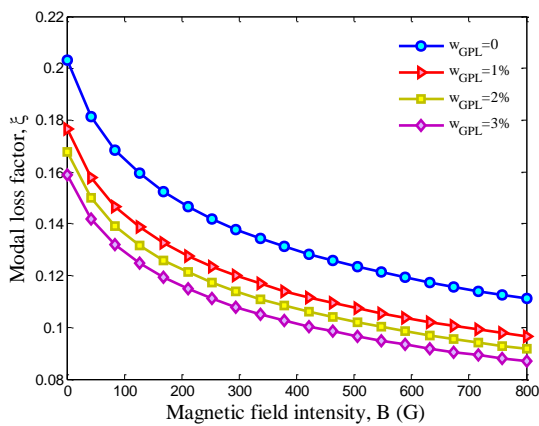


Fig. 10 Weight percent effect of the GPLs on the loss factor

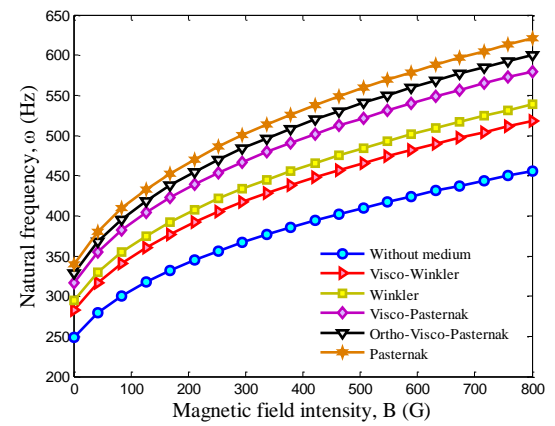


Fig. 13 Viscoelastic medium effect on the vibration

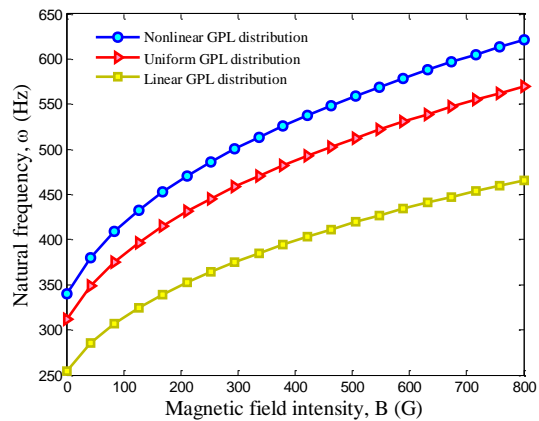


Fig. 11 The distribution effect of GPLs on the vibration

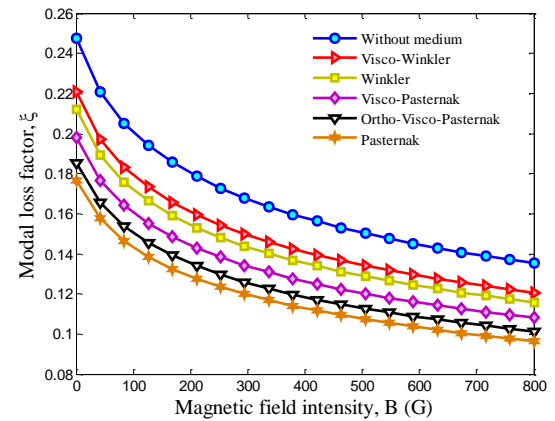


Fig. 14 Viscoelastic medium effect on the modal loss factor

at highest and the lowest values, respectively and the variation of the loss factor is vice versa. However, it can be expressed that the highest stiffness occurred when the distribution of GPLs is near to the inner and outer surfaces of the layer and when the distribution of GPLs is close to the neutral axis the worst case happens.

The influence of different types of viscoelastic mediums on the vibration and loss factor are plotted in Figs. 13 and 14. Six cases such as without medium, visco-Winkler, Winkler, visco-Pasternak, ortho-visco-Pasternak and

Pasternak mediums are analyzed. It is apparent that the vibration of the structure surrounded by Pasternak medium is occurred at higher frequencies in comparison with Winkler foundation but the loss factor is inverse. Furthermore, the vibration shifts to downward based on visco medium in comparison with non-visco medium. In addition, the vibration of the orthotropic medium occurs at lower frequencies with respect to the non-orthotropic medium.

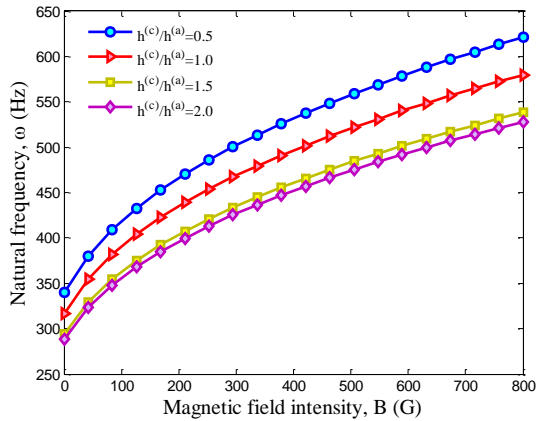


Fig. 15 The influence of the MR fluid to actuator thickness ratio on the vibration

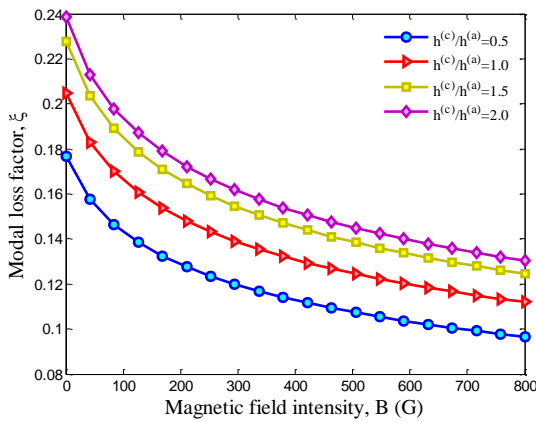


Fig. 16 The influence of the MR fluid to actuator thickness ratio on the loss factor

The influence of the thickness ratio ( $h^{(c)}/h^{(a)}$ ) on the vibration and loss factor is shown in Figs. 15 and 16. As it is obvious, lower frequency and upper loss factor occur by increasing the thickness ratio of MR fluid to actuator. In fact, the DIR moves to downward with increasing ratio thickness of MR fluid and actuator. It is because that by increasing MR fluid thickness, the damping effect of structure grows up and causes more stiffness for system.

Figs. 17 and 18 demonstrate the effect of the external voltage ( $V_0$ ) to the actuator layer on the vibration and loss factor. It is understood that negative voltages grow the vibration of the structure and positive voltages effect vice versa. The reason is that positive voltage enforces compressive forces to the structure but negative voltage performs tensile forces.

## 6. Conclusions

MR fluids are high-tech materials that can shift their phase from liquid to solid under external magnetic field and have remarkable potential in applications for intelligent systems, therefore, analyze the behavior of the is essential. This work investigates the control of vibration and damping of a sandwich structure with MR fluid core contain of

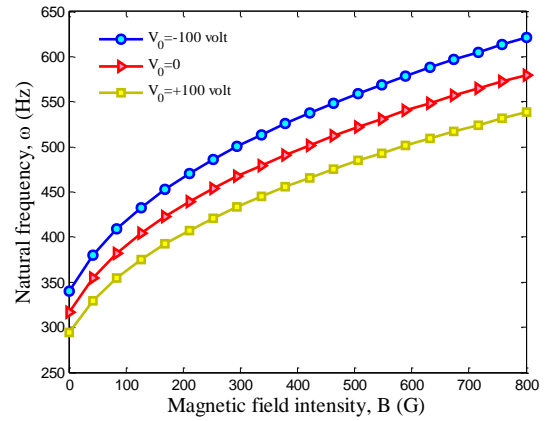


Fig. 17 Voltage effect on the vibration of the system

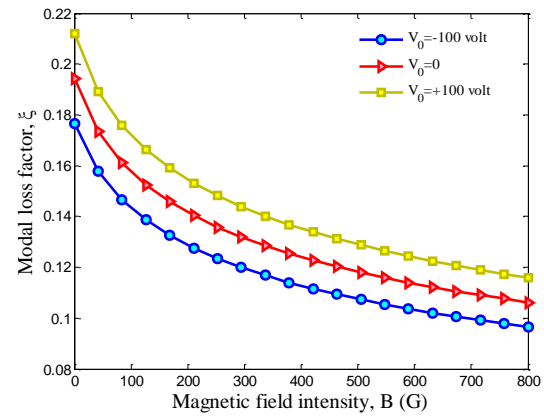


Fig. 18 Voltage effect on the loss factor of the system

piezoelectric layers as sensor and actuator. Halpin-Tsai model is used to determine the material properties of facesheets which are reinforced by GPLs. In addition, the MR fluid core and facesheets are subjected to magnetic field and 3D electric filed, respectively. Motion equations are derived according to SSDT and vibration of the structure is defined by DCM and Bolotin's method. The effect of different factors such as GPLs distribution, dimensions of structure, electro-magnetic field, damping of structure, viscoelastic environment and boundary conditions of the structure on the vibration and loss factor of the system were considered. Based on the above mentioned results, existence of PD controller and magnetic field enhance the vibration of the structure. Vibration occurs at higher and lower frequencies by performing negative and positive voltages. Furthermore, lower frequency and upper loss factor occur by increasing the thickness ratio of MR fluid to actuator. Moreover, for the nonlinear and linear GPLs distributions, the vibration of the system occurs at highest and the lowest values, respectively.

## References

- Abad, F. and Rouzegar, J. (2017), "An exact spectral element method for free vibration analysis of FG plate integrated with

- piezoelectric layers", *Compos. Struct.*, **180** 696-708.  
<https://doi.org/10.1016/j.compstruct.2017.08.030>
- Adiyaman, G., Yaylacı, M. and Birinci, A. (2015), "Analytical and finite element solution of a receding contact problem", *Struct. Eng Mech., Int. J.*, **54**(1), 69-85.  
<https://doi.org/10.12989/sem.2015.54.1.069>
- Adiyaman, G., Birinci, A., Öner, E. and Yaylacı, M. (2016), "A receding contact problem between a functionally graded layer and two homogeneous quarter planes", *Acta Mech.*, **227**(6), 1753-1766. <https://doi.org/10.1007/s00707-016-1580-y>
- Aguib, S., Nour, A., Zahloul, H., Bossis, G., Chevalier, Y. and Lançon, P. (2014), "Dynamic behavior analysis of a magnetorheological elastomer sandwich plate", *Int. J. Mech. Sci.*, **87** 118-136.  
<https://doi.org/10.1016/j.ijmecsci.2014.05.014>
- Birinci, A., Adiyaman, G., Yaylacı, M. and Öner, E. (2015), "Analysis of continuous and discontinuous cases of a contact problem using analytical method and FEM", *Latin Am. J. Solids Struct.*, **12**(9), 1771-1789.  
<http://dx.doi.org/10.1590/1679-78251574>
- Chen, C.-S., Liu, F.-H. and Chen, W.-R. (2017), "Vibration and stability of initially stressed sandwich plates with FGM face sheets in thermal environments", *Steel Compos. Struct., Int. J.*, **23**(3), 251-261. <http://dx.doi.org/10.12989/scs.2017.23.3.251>
- Eshaghi, M., Sedaghati, R. and Rakheja, S. (2016), "Analytical and experimental free vibration analysis of multi-layer MR-fluid circular plates under varying magnetic flux", *Compos. Struct.*, **157**, 78-86.  
<https://doi.org/10.1016/j.compstruct.2016.08.024>
- Güth, D. and Maas, J. (2016), "Long-term stable magnetorheological fluid brake for application in wind turbines", *J. Intellig. Mater. Syst. Struct.*, **27**(15), 2125-2142.  
<https://doi.org/10.1177/1045389X15624794>
- Hajmohammad, M.H., Zarei, M.S., Nouri, A. and Kolahchi, R. (2017), "Dynamic buckling of sensor/functionally graded-carbon nanotube-reinforced laminated plates/actuator based on sinusoidal-visco-piezoelectricity theories", *J. Sandw. Struct. Mat.*, 1-33. <https://doi.org/10.1177/1099636217720373>
- Hajmohammad, M.H., Farrokhan, A. and Kolahchi, R. (2018), "Smart control and vibration of viscoelastic actuator-multiphase nanocomposite conical shells-sensor considering hygrothermal load based on layerwise theory", *Aerosp. Sci. Technol.*, **78**, 260-270. <https://doi.org/10.1016/j.ast.2018.04.030>
- Han, Y., Wang, P., Fan, H., Sun, F., Chen, L. and Fang, D. (2015), "Free vibration of CFRC lattice-core sandwich cylinder with attached mass", *Compos. Sci. Technol.*, **118**, 226-235.  
<https://doi.org/10.1016/j.compscitech.2015.09.007>
- Jamali, M., Shojae, T., Kolahchi, R. and Mohammadi, B. (2016), "Buckling analysis of nanocomposite cut out plate using domain decomposition method and orthogonal polynomials", *Steel Compos. Struct., Int. J.*, **22**(3), 691-712.  
<https://doi.org/10.12989/scs.2016.22.3.691>
- Katariya, P.V. and Panda, S.K. (2019a), "Frequency and Deflection Responses of Shear Deformable Skew Sandwich Curved Shell Panel: A Finite Element Approach", *Arab. J. Sci. Eng.*, **44**(2), 1631-1648. <https://doi.org/10.1007/s13369-018-3633-0>
- Katariya, P.V. and Panda, S.K. (2019b), "Numerical evaluation of transient deflection and frequency responses of sandwich shell structure using higher order theory and different mechanical loadings", *Eng. Comput.*, **35**(3), 1009-1026.  
<https://doi.org/10.1007/s00366-018-0646-y>
- Katariya, P.V., Panda, S.K., Hirwani, C.K., Mehar, K. and Thakare, O. (2017a), "Enhancement of thermal buckling strength of laminated sandwich composite panel structure embedded with shape memory alloy fibre", *Smart Struct. Syst., Int. J.*, **20**(5), 595-605. <https://doi.org/10.12989/sss.2017.20.5.595>
- Katariya, P.V., Panda, S.K. and Mahapatra, T.R. (2017b), "Prediction of nonlinear eigenfrequency of laminated curved sandwich structure using higher-order equivalent single-layer theory", *J. Sandw. Struct. Mater.*, 1099636217728420.  
<https://doi.org/10.1177/1099636217728420>
- Katariya, P.V., Panda, S.K. and Mahapatra, T.R. (2018), "Bending and vibration analysis of skew sandwich plate", *Aircraft. Eng. Aerosp. Technol.*, **90**(6), 885-895.  
<https://doi.org/10.1108/AEAT-05-2016-0087>
- Kolahchi, R. (2017), "A comparative study on the bending, vibration and buckling of viscoelastic sandwich nano-plates based on different nonlocal theories using DC, HDQ and DQ methods", *Aerosp. Sci. Tech.*, **66**, 235-248.  
<https://doi.org/10.1016/j.ast.2017.03.016>
- Kolahchi, R. and Cheraghbak, A. (2017), "Agglomeration effects on the dynamic buckling of viscoelastic microplates reinforced with SWCNTs using Bolotin method", *Nonlinear Dyn.*, **90**(1), 479-492. <https://doi.org/10.1007/s11071-017-3676-x>
- Kolahchi, R., Hosseini, H. and Esmailpour, M. (2016), "Differential cubature and quadrature-Bolotin methods for dynamic stability of embedded piezoelectric nanoplates based on visco-nonlocal-piezoelectricity theories", *Compos. Struct.*, **157**, 174-186. <https://doi.org/10.1016/j.compstruct.2016.08.032>
- Kolahchi, R., Keshtegar, B. and Fakhar, M.H. (2017a), "Optimization of dynamic buckling for sandwich nanocomposite plates with sensor and actuator layer based on sinusoidal-visco-piezoelectricity theories using Grey Wolf algorithm", *J. Sandw. Struct. Mat.*, 1-25.  
<https://doi.org/10.1177/1099636217731071>
- Kolahchi, R., Zarei, M.S., Hajmohammad, M.H. and Nouri, A. (2017b), "Wave propagation of embedded viscoelastic FG-CNT-reinforced sandwich plates integrated with sensor and actuator based on refined zigzag theory", *Int. J. Mech. Sci.*, **130**, 534-545. <https://doi.org/10.1177/1099636217720373>
- Lall, A.K., Asnani, N.T. and Nakra, B.C. (1987), "Vibration and Damping Analysis of Rectangular Plate With Partially Covered Constrained Viscoelastic Layer", *J. Vib. Acoust. Stress Reliab.*, **109**(3), 241-247. <https://doi.org/10.1115/1.3269427>
- Lei, Y., Adhikari, S. and Friswell, M.I. (2013), "Vibration of nonlocal Kelvin-Voigt viscoelastic damped Timoshenko beams", *Int. J. Eng. Sci.*, **66-67**, 1-13.  
<https://doi.org/10.1016/j.ijengsci.2013.02.004>
- MalekzadehFard, K., Gholami, M., Reshadi, F. and Livani, M. (2015), "Free vibration and buckling analyses of cylindrical sandwich panel with magneto rheological fluid layer", *J. Sandw. Struct. Mat.*, **19**(4), 397-423.  
<https://doi.org/10.1177/1099636215603034>
- Mehar, K., Panda, S.K. and Patle, B.K. (2018), "Stress, deflection, and frequency analysis of CNT reinforced graded sandwich plate under uniform and linear thermal environment: A finite element approach", *Polym. Compos.*, **39**(10), 3792-3809.  
<https://doi.org/10.1002/pc.24409>
- Navazi, H.M., Bornassi, S. and Haddadpour, H. (2017), "Vibration analysis of a rotating magnetorheological tapered sandwich beam", *Int. J. Mech. Sci.*, **122** 308-317.  
<https://doi.org/10.1016/j.ijmecsci.2017.01.016>
- Nayak, B., Dwivedy, S.K. and Murthy, K.S.R.K. (2014), "Dynamic stability of a rotating sandwich beam with magnetorheological elastomer core", *Eur. J. Mech. A. Solids*, **47**, 143-155. <https://doi.org/10.1016/j.euromechsol.2014.03.004>
- Nguyen, T.-K., Thai, T. and Vo, T. (2015), "A refined higher-order shear deformation theory for bending, vibration and buckling analysis of functionally graded sandwich plates", *Steel Compos. Struct., Int. J.*, **18**(1), 91-120.  
<http://dx.doi.org/10.12989/scs.2015.18.1.091>
- Öner, E., Yaylacı, M. and Birinci, A. (2014), "Solution of a receding contact problem using an analytical method and a

- finite element method", *J. Mech. Mater. Struct.*, **9**(3), 333-345.  
<https://doi.org/10.2140/jomms.2014.9.333>
- Oveisi, A. and Nestorović, T. (2016), "Transient Response of an Active Nonlinear Sandwich Piezolaminated Plate", *Commun. Nonlin. Sci. Num. Sim.*, **45**, 158-175.  
<https://doi.org/10.1016/j.cnsns.2016.09.012>
- Sadeghpour, E., Sadighi, M. and Ohadi, A. (2016), "Free vibration analysis of a debonded curved sandwich beam", *Eur. J. Mech. A. Solids*, **57**, 71-84.  
<https://doi.org/10.1016/j.euromechsol.2015.11.006>
- Sekkal, M., Fahsi, B., Tounsi, A. and Hassan, S. (2017), "A novel and simple higher order shear deformation theory for stability and vibration of functionally graded sandwich plate", *Steel Compos. Struct.*, **25**, 389-401.  
<http://dx.doi.org/10.12989/scs.2017.25.4.389>
- Sharma, A., Kumar, A., Susheel, C.K. and Kumar, R. (2016), "Smart damping of functionally graded nanotube reinforced composite rectangular plates", *Compos. Struct.*, **155**, 29-44.  
<https://doi.org/10.1016/j.compstruct.2016.07.079>
- Sharma, N., Mahapatra, T.R., Panda, S.K. and Mehar, K. (2018), "Evaluation of vibroacoustic responses of laminated composite sandwich structure using higher-order finite-boundary element model", *Steel Compos. Struct., Int. J.*, **28**(5), 629-639.  
<https://doi.org/10.12989/scs.2018.28.5.629>
- Singh, V.K., Mahapatra, T.R. and Panda, S.K. (2016), "Nonlinear transient analysis of smart laminated composite plate integrated with PVDF sensor and AFC actuator", *Compos. Struct.*, **157**, 121-130. <https://doi.org/10.1016/j.compstruct.2016.08.020>
- Vescovini, R., D'Ottavio, M., Dozio, L. and Polit, O. (2018), "Buckling and wrinkling of anisotropic sandwich plates", *Int. J. Eng. Sci.*, **130**, 136-156.  
<https://doi.org/10.1016/j.ijengsci.2018.05.010>
- Wang, B., Liu, Y. and Xiao, Z. (2001), "Dynamical modelling of the chain structure formation in electrorheological fluids", *Int. J. Eng. Sci.*, **39**(4), 453-475.  
[https://doi.org/10.1016/S0020-7225\(00\)00054-9](https://doi.org/10.1016/S0020-7225(00)00054-9)
- Xu, J., Wang, P., Pang, H., Wang, Y., Wu, J., Xuan, S. and Gong, X. (2018), "The dynamic mechanical properties of magnetorheological plastomers under high strain rate", *Compos. Sci. Technol.*, **159**, 50-58.  
<https://doi.org/10.1016/j.compscitech.2018.02.030>
- Yang, B., Yang, J. and Kitipornchai, S. (2017), "Thermoelastic analysis of functionally graded graphene reinforced rectangular plates based on 3D elasticity", *Meccanica*, **52**(10), 2275-2292.  
<https://doi.org/10.1007/s11012-016-0579-8>
- Yaylaci, M. and Birinci, A. (2013), "The receding contact problem of two elastic layers supported by two elastic quarter planes", *Struct. Eng. Mech., Int. J.*, **48**(2), 241-255.  
<https://doi.org/10.12989/sem.2013.48.2.241>
- Yaylaci, M. and Birinci, A. (2015), "Analytical solution of a contact problem and comparison with the results from FEM", *Struct. Eng. Mech., Int. J.*, **54**(4), 607-622.  
<https://doi.org/10.12989/sem.2015.54.4.607>
- Yeh, J.-Y. (2011), "Free vibration analysis of rotating polar orthotropic annular plate with ER damping treatment", *Composites Part B*, **42**(4), 781-788.  
<https://doi.org/10.1016/j.compositesb.2011.01.023>
- Yeh, J.-Y. (2013), "Vibration analysis of sandwich rectangular plates with magnetorheological elastomer damping treatment", *Smart. Mater. Struct.*, **22**(3), 035010.  
<https://doi.org/10.1088/0964-1726/22/3/035010>
- Yeh, J.-Y., Chen, J.-Y., Lin, C.-T. and Liu, C.-Y. (2009), "Damping and vibration analysis of polar orthotropic annular plates with ER treatment", *J. Sound Vib.*, **325**(1), 1-13.  
<https://doi.org/10.1016/j.jsv.2009.02.047>
- Ying, Z., Chen, H. and Ni, Y. (2011), "Magnetorheological visco-elastomer and its application to suppressing microvibration of sandwich plates", *Proceedings of SPIE - The International Society for Optical Engineering*, **8409**, 42.  
<https://doi.org/10.1117/12.919835>
- Zarei, M.S., Azizkhani, M.B., Hajmohammad, M.H. and Kolahchi, R. (2017), "Dynamic buckling of polymer-carbon nanotube-fiber multiphase nanocomposite viscoelastic laminated conical shells in hygrothermal environments", *J. Sandw. Struct. Mat.*, 1-26. <https://doi.org/10.1177>

CC



where

$$\begin{aligned} & (A_{11}^{(a)}, A_{12}^{(a)}, A_{13}^{(a)}, A_{44}^{(a)}, A_{55}^{(a)}, A_{66}^{(a)}) \\ &= \int_{h^{(c)}/2}^{h^{(c)}/2+h^{(a)}} (Q_{11}^{(a)}, Q_{12}^{(a)}, Q_{13}^{(a)}, Q_{44}^{(a)}, Q_{55}^{(a)}, Q_{66}^{(a)}) dz, \end{aligned} \quad (A14)$$

$$\begin{aligned} & (A_{11}^{(s)}, A_{12}^{(s)}, A_{13}^{(s)}, A_{44}^{(s)}, A_{55}^{(s)}, A_{66}^{(s)}) \\ &= \int_{-h^{(c)}/2}^{-h^{(c)}/2-h^{(s)}} (Q_{11}^{(s)}, Q_{12}^{(s)}, Q_{13}^{(s)}, Q_{44}^{(s)}, Q_{55}^{(s)}, Q_{66}^{(s)}) dz, \end{aligned} \quad (A15)$$

$$\begin{aligned} & (B_{11}^{(a)}, B_{12}^{(a)}, B_{13}^{(a)}, B_{66}^{(a)}) \\ &= \int_{h^{(c)}/2}^{h^{(c)}/2+h^{(a)}} (Q_{11}^{(a)}, Q_{12}^{(a)}, Q_{13}^{(a)}, Q_{66}^{(a)}) z dz, \end{aligned} \quad (A16)$$

$$\begin{aligned} & (B_{11}^{(s)}, B_{12}^{(s)}, B_{13}^{(s)}, B_{66}^{(s)}) \\ &= \int_{-h^{(c)}/2}^{-h^{(c)}/2-h^{(s)}} (Q_{11}^{(s)}, Q_{12}^{(s)}, Q_{13}^{(s)}, Q_{66}^{(s)}) z dz, \end{aligned} \quad (A17)$$

$$\begin{aligned} & (D_{11}^{(a)}, D_{12}^{(a)}, D_{66}^{(a)}) \\ &= \int_{h^{(c)}/2}^{h^{(c)}/2+h^{(a)}} (Q_{11}^{(a)}, Q_{12}^{(a)}, Q_{66}^{(a)}) z^2 dz, \end{aligned} \quad (A18)$$

$$(D_{11}^{(s)}, D_{12}^{(s)}, D_{66}^{(s)}) = \int_{-h^{(c)}/2}^{-h^{(c)}/2-h^{(s)}} (Q_{11}^{(s)}, Q_{12}^{(s)}, Q_{66}^{(s)}) z^2 dz, \quad (A19)$$

$$\begin{aligned} & (G_{11}^{(a)}, G_{12}^{(a)}, G_{13}^{(a)}, G_{66}^{(a)}) \\ &= \int_{h^{(c)}/2}^{h^{(c)}/2+h^{(a)}} (Q_{11}^{(a)}, Q_{12}^{(a)}, Q_{13}^{(a)}, Q_{66}^{(a)}) f(z) dz, \end{aligned} \quad (A20)$$

$$\begin{aligned} & (G_{11}^{(s)}, G_{12}^{(s)}, G_{13}^{(s)}, G_{66}^{(s)}) \\ &= \int_{-h^{(c)}/2}^{-h^{(c)}/2-h^{(s)}} (Q_{11}^{(s)}, Q_{12}^{(s)}, Q_{13}^{(s)}, Q_{66}^{(s)}) f(z) dz, \end{aligned} \quad (A21)$$

$$\begin{aligned} & (H_{11}^{(a)}, H_{12}^{(a)}, H_{13}^{(a)}, H_{23}^{(a)}, H_{33}^{(a)}) \\ &= \int_{h^{(c)}/2}^{h^{(c)}/2+h^{(a)}} (Q_{11}^{(a)}, Q_{12}^{(a)}, Q_{13}^{(a)}, Q_{23}^{(a)}, Q_{33}^{(a)}) g'(z) dz, \end{aligned} \quad (A22)$$

$$\begin{aligned} & (H_{11}^{(s)}, H_{12}^{(s)}, H_{13}^{(s)}, H_{23}^{(s)}, H_{33}^{(s)}) \\ &= \int_{-h^{(c)}/2}^{-h^{(c)}/2-h^{(s)}} (Q_{11}^{(s)}, Q_{12}^{(s)}, Q_{13}^{(s)}, Q_{23}^{(s)}, Q_{33}^{(s)}) g'(z) dz, \end{aligned} \quad (A23)$$

$$\begin{aligned} & (I_{11}^{(a)}, I_{12}^{(a)}, I_{66}^{(a)}) \\ &= \int_{h^{(c)}/2}^{h^{(c)}/2+h^{(a)}} (Q_{11}^{(a)}, Q_{12}^{(a)}, Q_{66}^{(a)}) z f(z) dz, \end{aligned} \quad (A24)$$

$$\begin{aligned} & (I_{11}^{(s)}, I_{12}^{(s)}, I_{66}^{(s)}) \\ &= \int_{-h^{(c)}/2}^{-h^{(c)}/2-h^{(s)}} (Q_{11}^{(s)}, Q_{12}^{(s)}, Q_{66}^{(s)}) z f(z) dz, \end{aligned} \quad (A25)$$

$$\begin{aligned} & (J_{11}^{(a)}, J_{12}^{(a)}, J_{13}^{(a)}, J_{23}^{(a)}, J_{66}^{(a)}) \\ &= \int_{h^{(c)}/2}^{h^{(c)}/2+h^{(a)}} (Q_{11}^{(a)}, Q_{12}^{(a)}, Q_{13}^{(a)}, Q_{23}^{(a)}, Q_{66}^{(a)}) z g'(z) dz, \end{aligned} \quad (A26)$$

$$\begin{aligned} & (J_{11}^{(s)}, J_{12}^{(s)}, J_{13}^{(s)}, J_{23}^{(s)}, J_{66}^{(s)}) \\ &= \int_{-h^{(c)}/2}^{-h^{(c)}/2-h^{(s)}} (Q_{11}^{(s)}, Q_{12}^{(s)}, Q_{13}^{(s)}, Q_{23}^{(s)}, Q_{66}^{(s)}) z g'(z) dz, \end{aligned} \quad (A27)$$

$$\begin{aligned} & (K_{11}^{(a)}, K_{12}^{(a)}, K_{22}^{(a)}, K_{66}^{(a)}) \\ &= \int_{h^{(c)}/2}^{h^{(c)}/2+h^{(a)}} (Q_{11}^{(a)}, Q_{12}^{(a)}, Q_{22}^{(a)}, Q_{66}^{(a)}) f(z) g'(z) dz, \end{aligned} \quad (A28)$$

$$\begin{aligned} & (K_{11}^{(s)}, K_{12}^{(s)}, K_{22}^{(s)}, K_{66}^{(s)}) \\ &= \int_{-h^{(c)}/2}^{-h^{(c)}/2-h^{(s)}} (Q_{11}^{(s)}, Q_{12}^{(s)}, Q_{22}^{(s)}, Q_{66}^{(s)}) f(z) g'(z) dz, \end{aligned} \quad (A29)$$

$$\begin{aligned} & (L_{13}^{(a)}, L_{22}^{(a)}, L_{66}^{(a)}) \\ &= \int_{h^{(c)}/2}^{h^{(c)}/2+h^{(a)}} (Q_{13}^{(a)}, Q_{22}^{(a)}, Q_{66}^{(a)}) (g'(z))^2 dz, \end{aligned} \quad (A30)$$

$$\begin{aligned} & (L_{13}^{(s)}, L_{22}^{(s)}, L_{66}^{(s)}) \\ &= \int_{-h^{(c)}/2}^{-h^{(c)}/2-h^{(s)}} (Q_{13}^{(s)}, Q_{22}^{(s)}, Q_{66}^{(s)}) (g'(z))^2 dz, \end{aligned} \quad (A31)$$

$$(M_{44}^{(a)}, M_{55}^{(a)}) = \int_{h^{(c)}/2}^{h^{(c)}/2+h^{(a)}} (Q_{44}^{(a)}, Q_{55}^{(a)}) (g(z))^2 dz, \quad (A32)$$

$$(M_{44}^{(s)}, M_{55}^{(s)}) = \int_{-h^{(c)}/2}^{-h^{(c)}/2-h^{(s)}} (Q_{44}^{(s)}, Q_{55}^{(s)}) (g(z))^2 dz, \quad (A33)$$

$$\Psi^{(c)} = \int_{-h^{(c)}/2}^{h^{(c)}/2} G^* dz, \quad (A34)$$

$$\begin{aligned} & (E_{31}^{(a)}, E_{32}^{(a)}) \\ &= \int_{h^{(c)}/2}^{h^{(c)}/2+h^{(a)}} (e_{31}^{(a)}, e_{32}^{(a)}) \left( \frac{\pi}{h^{(a)}} \cos \left( \frac{\pi(z - h^{(c)}/2)}{h^{(a)}} \right) \right) dz, \end{aligned} \quad (A35)$$

$$\begin{aligned} & (E_{31}^{(s)}, E_{32}^{(s)}) \\ &= \int_{-h^{(c)}/2}^{-h^{(c)}/2-h^{(s)}} (e_{31}^{(s)}, e_{32}^{(s)}) \left( -\frac{\pi}{h^{(s)}} \cos \left( \frac{\pi(-z - h^{(c)}/2)}{h^{(s)}} \right) \right) dz, \end{aligned} \quad (A36)$$

$$\begin{aligned} & (F_{31}^{(a)}, F_{32}^{(a)}) \\ &= \int_{\frac{h^{(c)}}{2}}^{\frac{h^{(c)}}{2}+h^{(a)}} (e_{31}^{(P)}, e_{32}^{(P)}) \left( \frac{\pi}{h^{(a)}} \cos \left( \frac{\pi \left( z - \frac{h^{(c)}}{2} \right)}{h^{(a)}} \right) \right) dz \end{aligned} \quad (A37)$$

$$\begin{aligned} & (F_{31}^{(s)}, F_{32}^{(s)}) \\ &= \int_{-\frac{h^{(c)}}{2}}^{-\frac{h^{(c)}}{2}-h^{(s)}} (e_{31}^{(s)}, e_{32}^{(s)}) \left( -\frac{\pi}{h^{(s)}} \cos \left( \frac{\pi \left( -z - \frac{h^{(c)}}{2} \right)}{h^{(s)}} \right) \right) dz \end{aligned} \quad (A38)$$

$$\begin{aligned}
 & (E_{31}^{f(a)}, E_{32}^{f(a)}) \\
 &= \int_{h^{(c)}/2}^{h^{(c)}/2+h^{(a)}} (e_{31}^{(a)}, e_{32}^{(a)}) \left( \frac{\pi}{h^{(a)}} \cos \left( \frac{\pi(z - h^{(c)}/2)}{h^{(a)}} \right) \right) f(z) dz \quad (\text{A39})
 \end{aligned}$$

$$\begin{aligned}
 & (E_{31}^{f(s)}, E_{32}^{f(s)}) \\
 &= \int_{-h^{(c)}/2+h^{(s)}}^{-h^{(s)}/2} (e_{31}^{(s)}, e_{32}^{(s)}) \left( -\frac{\pi}{h^{(s)}} \cos \left( \frac{\pi(-z - h^{(c)}/2)}{h^{(s)}} \right) \right) f(z) dz \quad (\text{A40})
 \end{aligned}$$